Clim. Past, 19, 1321–1343, 2023
https://doi.org/10.5194/cp-19-1321-2023

Climate of the Past
Open Access
EGU

A High Arctic inner shelf–fjord system from the Last Glacial Maximum to the present: Bessel Fjord and southwest Dove Bugt, northeastern Greenland

Kevin Zoller[1], Jan Sverre Laberg[1], Tom Arne Rydningen[1], Katrine Husum[2], and Matthias Forwick[1]

[1]Department of Geosciences, UiT The Arctic University of Norway, Box 6050 Langnes, 9037 Tromsø, Norway
[2]Norwegian Polar Institute, Box 6606 Langnes, 9296 Tromsø, Norway

Correspondence: Kevin Zoller (kevin.zoller3@gmail.com)

Received: 22 September 2022 – Discussion started: 11 October 2022
Revised: 19 May 2023 – Accepted: 23 May 2023 – Published: 10 July 2023

Abstract. The Greenland Ice Sheet (GrIS) responds rapidly to the present climate; therefore, its response to the predicted future warming is of concern. To learn more about the impact of future climatic warming on the ice sheet, decoding its behavior during past periods of warmer than present climate is important. However, due to the scarcity of marine studies reconstructing ice sheet conditions on the Northeast Greenland shelf and adjacent fjords, the timing of the deglaciation over marine regions and its connection to forcing factors remain poorly constrained. This includes data collected in fjords that encompass the Holocene thermal maximum (HTM), a period in which the climate was warmer than it is at present. This paper aims to use new bathymetric data and the analysis of sediment gravity cores to enhance our understanding of ice dynamics of the GrIS in a fjord and inner shelf environment as well as give insight into the timing of deglaciation and provide a palaeoenvironmental reconstruction of southwestern Dove Bugt and Bessel Fjord since the Last Glacial Maximum (LGM). North–south-oriented glacial lineations and the absence of pronounced moraines in southwest Dove Bugt, an inner continental shelf embayment (trough), suggest the southwards and offshore flow of Storstrømmen, the southern branch of the Northeast Greenland Ice Stream (NEGIS). Sedimentological data suggest that an ice body, theorized to be the NEGIS, may have retreated from the region slightly before $\sim$ 11.4 cal ka BP. The seabed morphology of Bessel Fjord, a fjord terminating in southern Dove Bugt, includes numerous basins separated by thresholds. The position of basin thresholds, which include some recessional moraines, suggest that the GrIS had undergone multiple halts or readvances during deglaciation, likely during one of the cold events identified in the Greenland Summit temperature records. A minimum age of 7.1 cal ka BP is proposed for the retreat of ice through the fjord to or west of its present-day position in the Bessel Fjord catchment area. This suggests that the GrIS retreated from the marine realm in Early Holocene, around the onset of the HTM in this region, a period when the mean July temperature was at least 2–3 °C higher than at present and remained at or west of this onshore position for the remainder of the Holocene. The transition from predominantly mud to muddy sand layers in a mid-fjord core at $\sim$ 4 cal ka BP may be the result of increased sediment input from nearby and growing ice caps. This shift may suggest that in the Late Holocene (Meghalayan), a period characterized by a temperature drop to modern values, ice caps in Bessel Fjord probably fluctuated with greater sensitivity to climatic conditions than the northeastern sector of the GrIS.

1 Introduction

Ice mass loss from the Greenland Ice Sheet (GrIS) has accelerated during the 21st century, making it the largest individual contributor to sea level rise (King et al., 2020). This introduction of a substantial quantity of fresh water may have ramifications for global ocean circulations and the climate (Rahmstorf et al., 2015). Approximately 12 % of the ice from the GrIS is transported to the coast through the Northeast Greenland Ice Stream (NEGIS) (Khan et al., 2014; Joughin

et al., 2001) and therefore has a substantial impact on the mass balance of the ice sheet and the potential to contribute to sea level rise. Currently, two of the three marine-terminating outlet glaciers that are supplied by the NEGIS are in retreat (Mouginot et al., 2015), where the southernmost branch, Storstrømmen in Dove Bugt (Fig. 1a and b), is currently in a building phase following a 1978–1984 surge (Khan et al., 2014; Reeh et al., 1994). While there are numerous studies on the current state of the NEGIS during the past decades to century, there is a scarcity of data concerning the position and dynamics of the ice stream and other local northeastern Greenland outlet glaciers on a multi-century to millennial scale over marine regions. Considering that the global mean temperature is expected to continue to rise (Stocker et al., 2013) and that the Arctic will experience an amplification effect (Cohen et al., 2014), looking to the past, especially during warmer than present periods (i.e., the Holocene thermal maximum (HTM)), may provide an important insight into the future behavior of the ice sheet.

Marine studies have found evidence for past advancement and retreat of the GrIS and NEGIS along the continental shelf offshore northeastern Greenland (Evans et al., 2009; Winkelmann et al., 2010; Arndt et al., 2015, 2017; Laberg et al., 2017; Arndt, 2018; Olsen et al., 2020; Syring et al., 2020; Davies et al., 2022; Hansen et al., 2022; Jackson et al., 2022). Geomorphological findings in Store Koldewey Trough ($\sim 76^\circ$ N), a major shelf trough northeast of the study area (Fig. 1b), suggests that the ice sheet may have reached the shelf break in this area during the LGM (Last Glacial Maximum) (Laberg et al., 2017; Olsen et al., 2020). However, further north ($\sim 79.4^\circ$ N), findings by Rasmussen et al. (2022) indicate that some regions near the shelf break were ice free during the LGM despite Arndt et al. (2017) positioning the ice front at its maximum LGM position at the outer shelf. A concise understanding of the timing and dynamics of the ice sheet over the Northeast (NE) Greenland shelf during the subsequent deglaciation of the marine realm remains to be established as very few dated cores have been recovered. Terrestrial dating (e.g., cosmogenic nuclide dates and lake studies) has provided further insight into when terrestrial regions had become deglaciated and how the climate has changed in these areas (e.g., Björck and Persson, 1981; Björck et al., 1994; Wagner et al., 2008; Klug et al., 2009a; Schmidt et al., 2011; Skov et al., 2020; Larsen et al., 2020). However, only recently have terrestrial data been integrated with marine data to establish a detailed deglaciation chronology of the shelf, coast, and fjord regions (Davies et al., 2022; Larsen et al., 2022).

Swath bathymetry and gravity cores data from southwestern Dove Bugt (i.e., Store Bælt) and Bessel Fjord (Fig. 1), presented for the first time in this study, has been used to further refine our understanding of how the GrIS responded to changes in palaeoclimatic conditions from the LGM through the Holocene, including the HTM. Through this analysis we aim to reconstruct regional ice dynamics from both full-glacial conditions and during overall retreat and put our findings into the larger context of the dynamics of the Northeast Greenland Ice Sheet during these periods. Additionally, this study aims to refine our understanding about the timing of deglaciation over marine areas and compare findings to nearby terrestrial regions including the Store Koldewey, Hochstetter Forland, and Shannon Ø. Results will also contribute to our understanding of palaeoenvironmental conditions throughout the Holocene for the NE Greenland fjords and inner shelf areas.

2 Regional setting and environmental history

Bessel Fjord is a west–east-running fjord between Adolf S. Jensen Land and Dronning Margrethe II Land (Fig. 1c). The western end of the fjord contains the southern outlet glacier Soranerbræen, which also has a second outlet to the north in a tributary fjord to inner Dove Bugt (Fig. 2). Several ice caps are positioned across the length of the fjord (Figs. 2 and 3), some of which have several generations of moraines and glaciofluvial outlets that enter the fjord. Colluvial fans and rivers have been observed across the length of the fjord in satellite images and while surveying the fjord. Multiple islands are located at the entrance of Bessel Fjord, the largest of which, Trums Ø, splits the entrance into two main inlets (Figs. 1c and 2). The region from the termination of Soranerbræen to the entrance of the fjord measures ~ 60 km in length. The width of the fjord ranges from 1.8 to 3.7 km.

To the west of Bessel Fjord and Soranerbræen is the larger glacier L. Bistrup Bræ, which flows northwards and has an outlet in Borgfjorden, another tributary fjord to inner Dove Bugt (Fig. 1). Here it is confluent with the southward-flowing NEGIS outlet glacier, Storstrømmen (Rignot et al., 2022). Studies of modern Soranerbræen, L. Bistrup Bræ and Storstrømmen suggest that they all have separate drainage basins (Krieger et al., 2020). Storstrømmen and L. Bistrup Bræ are two of the largest surge-type glaciers in the world (Higgins, 1991) with a surge periodicity of approximately 70 years (Mouginot et al., 2018).

Bathymetry of inner Dove Bugt and tributary fjords has revealed that there are no natural large passageways for the warm, salty, subsurface Atlantic Intermediate Water to impact these glaciers at present, therefore it has been suggested that ocean waters do not play a large role in the evolution of Storstrømmen, L. Bistrup Bræ and the northern outlet of Soranerbræen, and that their grounding line retreat is mostly caused by ice thinning (Rignot et al., 2022).

Mega-scale glacial lineations (MSGL) identified in Store Koldewey Trough on the continental shelf have been interpreted as evidence for the expanse of this sector of the GrIS to the shelf break during the LGM (Laberg et al., 2017; Olsen et al., 2020). This is further supported by the presence of recessional moraines and grounding zone wedges, which suggests a complex deglaciation of this part of the shelf area (Arndt et

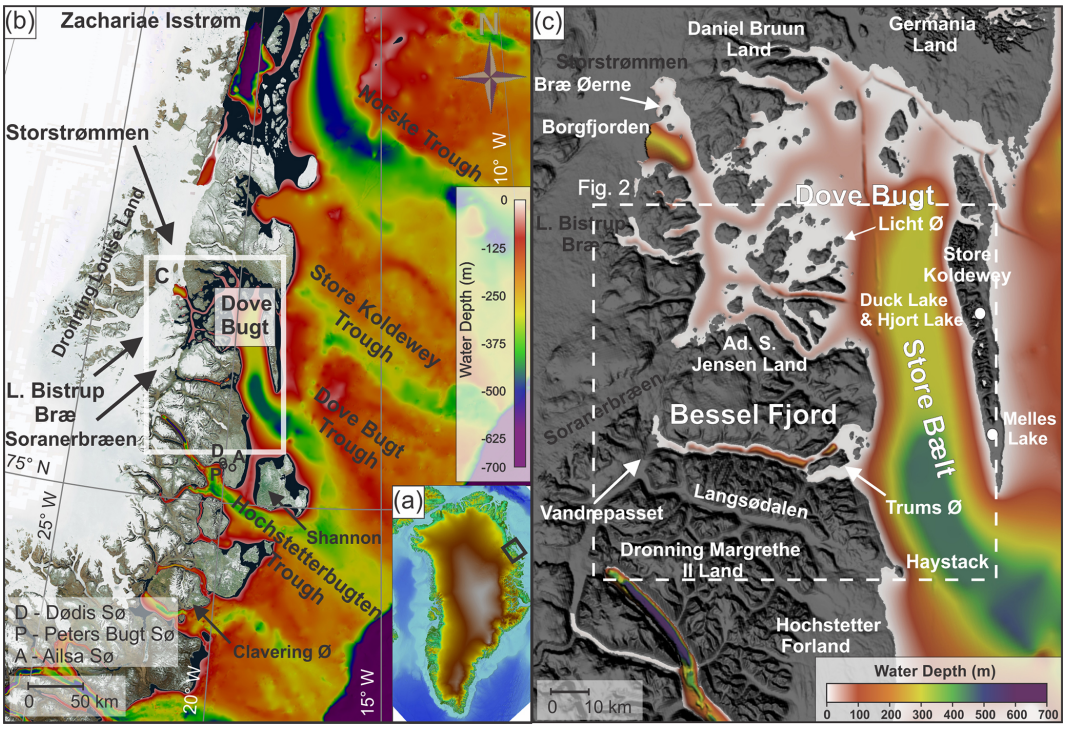

Figure 1. **(a)** An image of Greenland using IBCAO 4.0 400 × 400 m (Jakobsson et al., 2020) with a black box surrounding the study area. **(b)** Bathymetry of northeastern Greenland displayed using IBCAO 4.0 200 × 200 m data (Jakobsson et al., 2020), and land is displayed using a World Imagery satellite image (Earthstar Geographics, Esri, HERE, Garmin, FAO, NOAA, USGS) made available through GlobalMapper. The white box surrounds the position of Fig. 1c. **(c)** Bathymetry of Dove Bugt and Bessel Fjord and surrounding land areas displayed using the IBCAO 4.0 200 × 200 m data (Jakobsson et al., 2020). Locations mentioned in the text are labeled here. The position of Fig. 2 is within the dashed white box.

al., 2015, 2017; Laberg et al., 2017; Arndt, 2018; Olsen et al., 2020). Olsen et al. (2020) suggested that deglaciation in the Store Koldewey Trough may have occurred in two stages: an initial retreat as a result of eustatic sea level rise caused by melting ice at lower latitudes (Lambeck et al., 2014), followed by a melting phase driven by ocean warming. So far, the timing of the onset of the deglaciation is not known. Across the GrIS, deglaciation is believed to be asynchronous, with factors such as topography and local ice dynamics playing a large role in ice retreat in conjunction with climate change (Bennike and Björck, 2002; Funder et al., 2011; Ó Cofaigh et al., 2013; Hogan et al., 2016).

A recent study by Jackson et al. (2022) of the inner shelf east of the Clavering Ø (∼ 74° N; Fig. 1b) indicated that during the late Younger Dryas, this sector of the GrIS had reached a more landward position, in conformity with Funder et al. (2021). During this period, the inner shelf bottom water was characterized by anomalously high temperatures, interpreted to have played a role in the ice retreat and leading to the termination of the Younger Dryas stadial. This was followed by the onset of the East Greenland Current, as seen from cooler bottom water from the Early Holocene on Jackson et al. (2022).

Further north, east of marine-terminating glacier Zachariae Isstrøm (∼ 78° 30° N; Fig. 1b), the deglaciation of the NEGIS from the inner shelf was found to have occurred as early as 12.5 cal ka BP, likely before 13.4 cal ka BP (Davies et al., 2022). Here, inflow of warmer water (Atlantic Water) may have played a role. This part of the shelf was covered by an ice shelf from 13.4 to 11.2 cal ka BP (including the Younger Dryas), retreating and leading to open water conditions from the earliest Holocene at 11.2–10.8 cal ka BP, before readvancing from 10.8 to 9.6 cal ka BP, and finally retreating from 9.6 to 7.9 cal ka BP. At 7.9 cal ka BP there was a drastic shift in ocean circulation at this site with a sharp decline in Atlantic Water corresponding to an increase in Polar Water influx (Davies et al., 2022). Pados-Dibattista et al. (2022), studying another core from the NE Greenland shelf (more seaward, in a mid-shelf position north of the Norske Trough at ∼ 79° N), found that during the Early Holocene (9.4 to 8.2 cal ka BP) the East Greenland Current was highly stratified with cold surface water overlying warm Atlantic subsurface water. Following the 8.2 ka event, the interval from 8.2 to 6.2 cal ka BP was followed by the warmest Holocene bottom water conditions on the shelf. Afterwards, conditions returned to those seen prior to 8.2 cal ka BP due to increased Polar Water transport

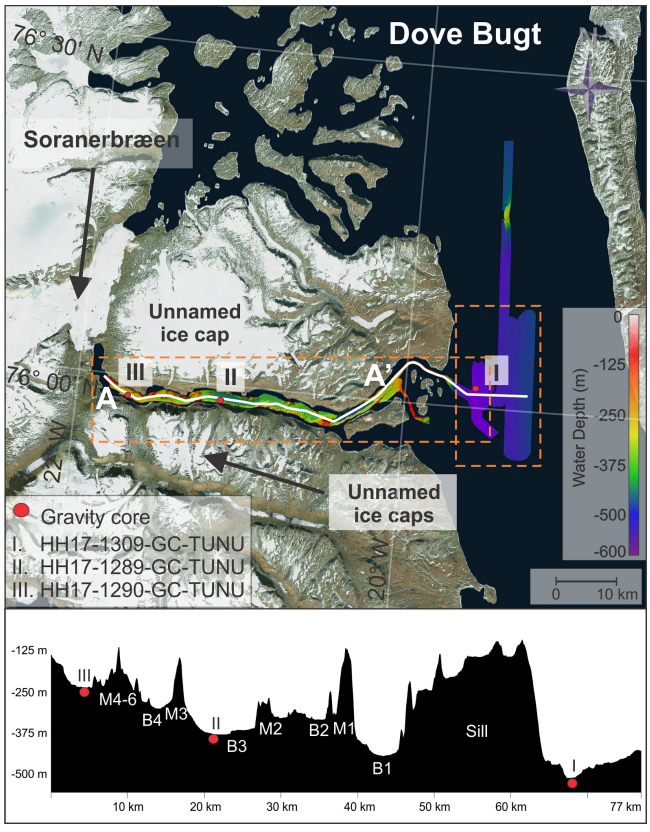

Figure 2. Study area with the bathymetric data showing the locations of the sediment cores presented in this study. The lower panel is a profile along the length of Bessel Fjord, A–A'. Sediment cores are labeled I, II, and III. The satellite image is displayed using a World Imagery satellite image (Earthstar Geographics, Esri, HERE, Garmin, FAO, NOAA, USGS) made available through Global Mapper.

strengthening the East Greenland Current (Pados-Dibattista et al., 2022).

Terrestrial studies of Dronning Margrethe II Land, Germania Land, and adjacent areas have identified a complex assortment of moraines that are believed to have formed during the Kap Mackenzie, Muschelbjerg, Nanok I, and Nanok II stadials (Hjort, 1979, 1981; Hjort and Björck, 1983; Björck et al., 1994; Landvik, 1994). The exact ages of these stadials remain unclear (Table 1), yet Larsen et al. (2022) suggest that Nanok stadial moraines found in Store Koldewey formed synchronously with the Milne Land moraines of Scoresby Sund, which date from the Allerød to early Younger Dryas and Preboreal periods (Kelly et al., 2008; Levy et al., 2016).

The position of striations on Store Koldewey and lateral moraines on coastal slopes between Bessel Fjord and Haystack have been interpreted as evidence for ice flowing out of Dove Bugt and Bessel Fjord during the Muschelbjerg stadial, southwards through Store Bælt and turning eastwards around the southernmost mountains of Store Koldewey (Hjort, 1981). Early studies of the region noted glacial

Table 1. Previously published stadial information for the Dove Bugt region and age estimates used in this study.

Stadials	Studies				Age estimate used in this study
	Hjort and Björck (1983)	Funder et al. (1998)	Kelly et al. (2008)	Vasskog et al. (2015)	Larsen et al. (2022)	
Nanok II	10.1–9.5 cal ka BP	Preboreal (ending at ca. 9.7 cal ka BP)	Younger Dryas and Early Holocene (13–11.6 ka (G-III), 11.7–10.6 ka (G II))	Close to Bølling–Allerød transition and late Younger Dryas (~ 14 cal ka BP (G III), ~ 12 cal ka BP (G-II))	Preboreal	Preboreal
Nanok I	Older than 14 cal ka BP, possibly between 15 and 19 cal ka BP				Late Allerød to early Younger Dryas	Late Allerød to early Younger Dryas
Nanok 0		~ 48 cal ka BP (Hjort, unpublished data)				?
Muschelbjerg	Saalian (or older)?					Saalian (or older)?
Kap Mackenzie	Saalian (or older)?					Saalian (or older)?

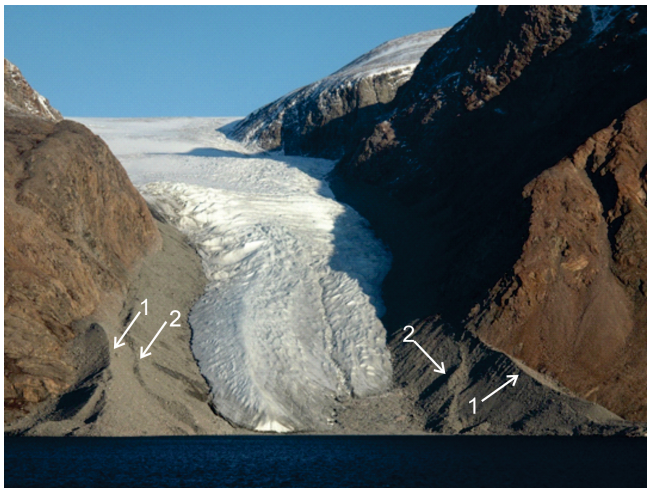

Figure 3. Image of an ice lobe from an ice cap near gravity core HH17-1289-GC-TUNU. Two sets of coarse-grained terminal morainic ridges are indicated by number and arrow. See Fig. 6b for the position of the modern ice lobe. The photograph was taken by Torger Grytå on a 2017 TUNU cruise.

and glaciofluvial deposits (e.g., moraine plateau, terminal moraines, eskers, and sandurs) on Hochstetter Forland that are believed to have formed during this period (Hjort, 1979, 1981).

Lateral moraines and glacial striations oriented along the axis of Langsödal (also referred to as Langsødalen; Fig. 1c), a nearby valley south of and sub-parallel to Bessel Fjord, have been interpreted as evidence for glacial confinement within the valley during an undifferentiated Nanok stadial (Hjort 1979, 1981). This differs from striations that have also been identified in the valley along more weathered surfaces that are oriented in a southwestern direction (Hjort, 1979).

The outer coastal regions of northern and northeastern Greenland are believed to have been deglaciated between 12.8 and 9.7 ka BP and present ice positions were reached between 10.8 to 5.8 ka BP (Larsen et al., 2022). Cosmogenic nuclide dates from Store Koldewey, first collected by Håkansson et al. (2007), and later Skov et al. (2020) and Larsen et al. (2022), suggest that ice retreated from the continental shelf and reached the upper and lower sections of the island by 12.3 and 12.7 ka BP, respectively. In contrast, Biette et al. (2020) found evidence of the deglaciation of Clavering Ø at 16.2 ka BP, with readvances at 11.3, 10.8, 3.3, 1.2, and 0.37 ka BP. Additional cosmogenic nuclide findings indicate that Trums Ø, in outer Bessel Fjord, may have become deglaciated around 12.6 ka BP, while Vandrepasset, onshore inner Bessel Fjord, may have become deglaciated by 8.6 ka BP (Larsen et al., 2022).

Findings from macrofossil remains (Bennike and Björck, 2002) and lacustrine sedimentary records (Cremer et al., 2008) suggest that coastal regions were deglaciated in a ∼ 1500-year span after the start of the Holocene (Klug et al., 2016). To the north of Store Koldewey, a minimum date for deglaciation in Germania Land of 9.5 cal ka BP has been proposed (Landvik, 1994), whereas to the south in southern Dronning Margrethe II Land, a minimum date of 11.2 cal ka BP has been suggested (Bennike and Weidick, 2001). Lake studies on aquatic organisms at Duck Lake and Hjort Lake on Store Koldewey (Fig. 1c) indicate that the island was at its warmest between ∼ 8 and 4 cal ka BP, (Wagner et al., 2008; Klug et al., 2009a; Schmidt et al., 2011), although findings from Melles Lake (Fig. 1c) suggest that the earliest onset of warmth during the Holocene may have occurred at ∼ 10 cal ka BP (Klug et al., 2009b; Briner et al., 2016). On Hochstetter Forland (Fig. 1c), pollen assemblages from Dødis Sø, Peters Bugt Sø, and Ailsa Sø suggest that the temperatures were at their highest between 8.8 and 5.6 cal ka BP (Björck and Persson, 1981; Björck et al., 1994). These findings indicate that the HTM was not uniform across eastern Greenland, as also described by Briner et al. (2016).

To the south, offshore the Kaiser Franz Josef Fjord system (∼ 73° N), a detailed biomarker record finds this part of the shelf dominated by seasonal sea ice throughout the Late Holocene (< ∼ 5 cal ka BP) and extended concentrations from 5.2 to 2.2 and 1.3 cal ka BP to present. Short-term variability was also seen for this area for the last 2.2 cal ka BP, corresponding to the climatic events of this period (Kolling et al., 2017).

3 Material and methods

Swath bathymetry and three sediment cores were collected in southwestern Dove Bugt and Bessel Fjord during an expedition aboard RV *Helmer Hanssen* of UiT The Arctic University of Norway in September 2017, being part of the TUNU program (Fig. 2; Christiansen, 2012). The swath bathymetry data was obtained using a Kongsberg Maritime Simrad EM 302 multibeam echo sounder. It was gridded using Petrel software, and geomorphological interpretations were made using Global Mapper 18. Surfaces were developed using a 5 × 5 m grid cell size, while a surface was created from an International Bathymetric Chart of the Arctic Ocean (IBCAO) dataset 4.0 with a 200 × 200 m grid cell size (Jakobsson et al., 2020).

Two soft sediment gravity cores were retrieved from Bessel Fjord (HH17-1289-GC-TUNU and HH17-1290-GC-TUNU) and one southwest of Dove Bugt in the sound Store Bælt (HH17-1309-GC-TUNU) (Fig. 2 and Table 2). Prior to splitting the cores, physical properties were measured using a GEOTEK Multi Sensor Core Logger (MSCL-S). The cores were placed in the laboratory for 24 h prior to obtaining physical measurements to ensure that each core temperature reached equilibrium with the laboratory to avoid distorting *p*-wave values (Weber et al., 1997).

A GEOTEK MSCL X-ray Computed Tomographic imaging machine was also used to scan the unopened core sec-

Table 2. Information on the position, water depth and recovery length of each gravity core. Note that the core names are abbreviated in the text.

Location	Inner Bessel Fjord	Mid-Bessel Fjord	Southeastern Dove Bugt
Coring station	HH17-1290	HH17-1289	HH17-1309
Latitude (N)	75°58′34.5907″	75°58′11.4928″	76°01′34.0387″
Longitude (W)	21°07′13.1055″	21°41′48.0278″	19°34′31.3190″
Water depth (m)	372	225	512
Recovery (cm)	534.5	245.5	474.55

tions to create X-ray radiographic images. After each core was split and cleaned, the characteristics of the sedimentary surface were logged (i.e., structures, bioturbation, grain size, lithological boundaries, etc.), sediment color was noted using the Munsell Soil Color Chart and lithofacies were assigned based on Eyles et al. (1983) classification system. Colored images of the core sections were then obtained using an Avaatech XRF core scanner.

Mollusks and benthic foraminifera were recovered from each core for the purpose of radiocarbon dating of lithofacies boundaries. This was, however, not always possible due to the low content of foraminifera and mollusks in these cores, which also restricted the number of dates that could be obtained. Two adjacent 1 cm thick sediment slices were successfully sampled from select positions across cores HH17-1290 and HH17-1309. Samples were then wet sieved at 1 mm, 100, and 63 µm meshes, respectively. Benthic foraminifera from the 100 µm size fraction were extracted for radiocarbon dating. Radiocarbon dating was carried out at the MICADAS radiocarbon laboratory at Alfred Wegener Institute, Helmholtz Centre for Polar and Marine Research, Germany. The radiocarbon dates were calibrated using the online version of OxCal 4.4 (ORAU, 2022) and the Marine20 calibration curve (Heaton et al., 2020), as the calibrated ^{14}C samples are younger than 11.5 cal ka BP (Heaton et al., 2022). We are using a ΔR of -10 ± 60 in conformity with Jackson et al. (2022). Previously reported radiocarbon dates from this area that are relevant to our study have been recalibrated using Marine20 for marine samples under 11.5 cal ka BP and IntCal20 for terrestrial samples (Reimer et al., 2020). One marine sample older than 11.5 cal ka BP has also been included (Table 3). In the Arctic, including our study area, calibration of marine samples by Marine20 is not recommended for samples older than 11.5 cal ka BP (see Heaton et al., 2022); therefore, this calibrated age is treated with caution.

A Beckman Coulter LS 13 320 Multi-Wavelength Laser Diffraction Particle Size Analyzer was used to perform sediment grain size analysis. Sediment was sampled in mostly 10 cm intervals across HH17-1309, where samples taken from the other two cores were selected from specific positions. Samples were treated in HCl and H_2O_2 and a preheated VWB 18 Thermal Bath. Samples were then cleaned using distilled water, placed through multiple runs through a centrifuge, and heated in an oven to remove water content. Approximately 0.2 g of sediment was then separated and placed in a container with 20 mL of water and moved to a shaking table for over 48 h. A few drops of Calgon were added to each sample, which was then placed into a Branson 200 ultrasonic cleaner for $\sim$ 7 min and shaken briefly before being poured through a $>$ 2 mm mesh and into the particle size analyzer. Grains between the size of 0.4 µm and 2000 µm were counted and underwent three separate runs. GRADISTAT Excel software was used to calculate the mean of the three runs. Sediment names used in reference to this analysis are based on Folk (1954) and mean grain size from the methodology published by Folk and Ward (1957).

4 Results

4.1 Seafloor landforms in SW Dove Bugt (Store Bælt)

4.1.1 Elongated lineations – glacial lineations

Slightly curved sub-parallel lineations, oriented sub-parallel to the axis of Dove Bugt, are the most pronounced landforms in this part of the study area. They are oriented N–NW in the south and N–NE in the north (Fig. 4). The most frequently identified positive lineations (ridges) are 35–50 m in width, $<$ 1–3 m in height, and between 1 and 10 km in length. Length-to-width ratios are frequently $>10:1$. At elevations shallower than 435 m depth, near the center of Store Bælt, the lineations are wider (e.g., 60–150 m wide), and occasional merging and overlapping of lineations occur (Fig. 4e). Wider lineations, often identified in the southern section of the study area (Fig. 4b), have also been identified with widths, lengths, and heights ranging from 200–650 m, 3–8 km, and 4.5–15 m, respectively. Length-to-width ratios here are $7:1$ to $>10:1$. Some of the larger lineations are superimposed by smaller lineations. Lateral ridges have also been identified in clusters overprinting the lineations (Fig. 4c), where furrows have been found cross-cutting lineations (Fig. 4d). Lateral ridges measure 0.5 to 2 m in height and are approximately 45 to 250 m apart.

These elongated lineations are interpreted as glacial lineations (e.g., Ó Cofaigh, 2005). The thinner, more common lineations (with length/width-ratios $>10:1$) have been in-

Table 3. Other published radiocarbon dates and their recalibrated ages using Marine20 (and an ΔR of -10 ± 60 in conformity with Jackson et al., 2022) and IntCal20 for aquatic moss samples. * The age of sample Lu-1298 from Shannon is above what is recommended by Heaton et al. (2022) for use with Marine20. This date was considered an outlier and therefore not taken into consideration by the authors and Bennike and Björck (2002). Therefore, this date is also rejected in the present study.

Location	Material	Lab no.	^{14}C age	^{14}C cal BP (1σ range)	^{14}C cal BP (median)	Reference
Shannon	shell	Lu-1298*	$19\,000 \pm 190$	21 855–22 325	22 078	Hjort (1981, 1979)
Hochstetter F.	shell	Lu-1289	9190 ± 90	9572–9926	9779	Hjort (1981, 1979)
Shannon	shell	Lu-1389	9370 ± 90	9865–10 195	10 015	Hjort (1981, 1979)
Hochstetter F.	shell	Lu-1386	9400 ± 90	9896–10 220	10 054	Hjort (1981, 1979)
Hochstetter F.	shell	Lu-1300:1	9470 ± 90	9970–10 322	10157	Hjort (1981, 1979)
Hochstetter F.	shell	Lu-1300:2	9520 ± 90	10 084–10 412	10 229	Hjort (1981, 1979)
Hochstetter F.	shell	Lu-1384	9810 ± 95	10 409–10 794	10617	Hjort (1981, 1979)
Ardencaple Fjord	shell	Lu-1390	8570 ± 85	8864–9200	9022	Hjort (1981, 1979)
Kildedalen	shell	Lu-1303	8930 ± 90	9290–9573	9447	Hjort (1981, 1979)
Snenæs	*Mya truncata, Hiatella arctica*	T-9372	8265 ± 95	8434–8768	8619	Landvik (1994)
Hvalrosodden moraine	*Nuculana pernula*	TUa-123	8685 ± 95	9006–9315	9166	Landvik (1994)
Hvalrosodden moraine	*Nuculana pernula*	TUa-124	9045 ± 90	9438–9741	9596	Landvik (1994)
Hvalrosodden	*Mya truncata*	T-9361	8190 ± 95	8360–8663	8523	Landvik (1994)
Hvalrosodden	*Mya truncata, Hiatella arctica*	T-9370	7930 ± 120	8681–9085	8890	Landvik (1994)
Hvalrosodden	*Mya truncata*	T-9371	7490 ± 115	8186–8502	8348	Landvik (1994)
Peters Bugt	*Portlandia arctica*	Ua-2787	$10\,260 \pm 105$	11 071–11 444	11 253	Björck et al. (1994)
Peters Bugt Sø	*Hiatella arctica*	Lu-3516	9640 ± 90	10 222–10 527	10 382	Björck et al. (1994)
Storstrømmen Sound	*Mya truncata*, *Hiatella arctica*	K-6098	5180 ± 95	5220–5520	5352	Weidick et al. (1994)
Storstrømmen Sound	*Mya truncata*	K-5494	4910 ± 85	4865–5175	5028	Weidick et al. (1994)
Storstrømmen Sound	*Mya truncata*	K-5493	4840 ± 90	4793–5117	4943	Weidick et al. (1994)
Storstrømmen Sound	*Hiatella arctica*	Ua-3347	5030 ± 75	5023–5311	5166	Weidick et al. (1994)
Storstrømmen Sound	*Hiatella arctica*	Ua-3350	4180 ± 60	3944–4225	4082	Weidick et al. (1994)
Storstrømmen Sound	*Balanoptera physalus*	K-6096	3630 ± 90	3230–3530	3380	Weidick et al. (1994)
Storstrømmen Sound	*Hiatella arctica*	Ua-3349	3725 ± 60	3371–3616	3496	Weidick et al. (1994)
Storstrømmen Sound	*Hiatella arctica*, *Mya truncata*	K-6097	3230 ± 85	2749–3024	2897	Weidick et al. (1994)
Storstrømmen Sound	*Hiatella arctica*	Ua-3348	1815 ± 55	1115–1317	1217	Weidick et al. (1994)
Hjort Lake	*Warnstorfia exannulata*	Poz-6194	8260 ± 50	8456–8722	8602	Wagner et al. (2008)
Duck Lake	Aquatic moss	LuS-6525	8690 ± 230	9527–10145	9775	Klug et al. (2009a)

terpreted as mega-scale glacial lineations (MSGL), and such landforms are commonly associated with palaeo-ice-stream environments (e.g., Stokes and Clark, 2001). Glacial lineations have been identified in numerous continental shelf regions around Greenland (Evans et al., 2009; Dowdeswell et al., 2014; Slabon et al., 2016; Laberg et al., 2017; Newton et al., 2017; Arndt, 2018; Batchelor et al., 2018; Jakobsson et al., 2018). While the mechanisms behind the formation of these features are still being debated, some authors have suggested that they may have formed through meltwater flooding (Shaw et al., 2008), groove-plowing (Clark et al., 2003) or the transverse flow in basal ice (Schoof and Clarke, 2008). King et al. (2009) favored aspects of the dilatant till instability model that could explain the development of MSGLs on a decadal timescale. Sets of ridges that overprint the glacial lineations have been interpreted as recessional moraines, where furrows have been interpreted as iceberg plow marks.

4.1.2 Depression and mound – hill–hole pair

In northern Store Bælt, a 200 by 450 m wide, 3–4 m deep depression has been identified next to a mound with a width and height of 235 by 450 and 3–4 m, respectively (Fig. 4d). The depression overprints N–S-trending lineations, although the mound contains lineations on its surface.

This depression and mound have been interpreted as a hill–hole pair. These landforms can form when ice-thrust rafts of sediment are removed from the bed by cold-based, slow-flowing ice that transports the sediment that was once in the depression (Hogan et al., 2010; Klages et al., 2013, 2015). In this instance, a south bound ice stream may have removed frozen sedimentary material and deposited it further south. This interpretation is in conformity with studies from other high-latitude continental shelves where subglacial hill–hole pairs are interpreted as being formed by ice frozen to the seafloor bed (Sættem, 1990; Ottesen et al., 2005).

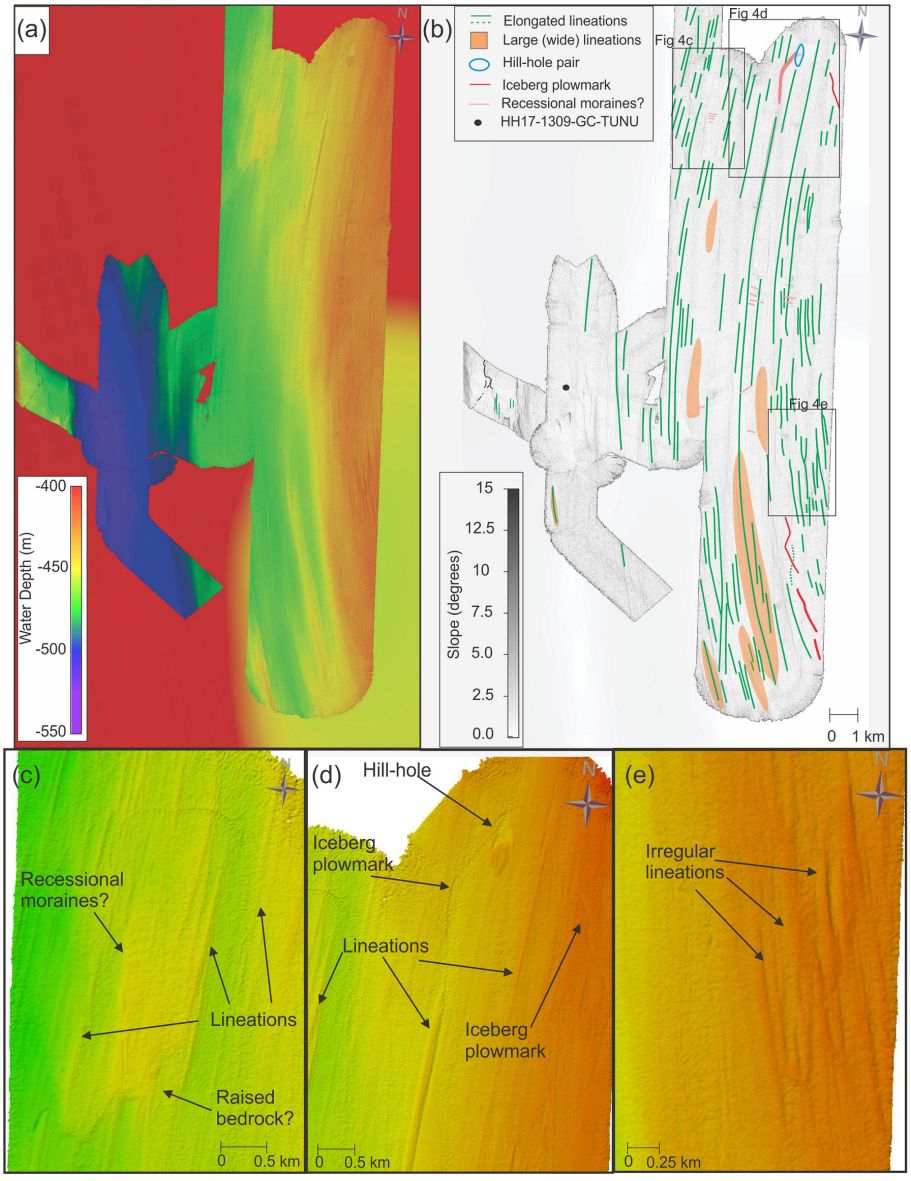

Figure 4. Bathymetric maps from SW Dove Bugt. **(a)** Seafloor relative to water depth with IBCAO 4.0 displayed in the background (Jakobsson et al., 2020). **(b)** The main landforms and slope angles of the seafloor in SW Dove Bugt. Locations of **(c)**–**(e)** are indicated. **(c)** Bathymetry of the northwestern section of the study area. **(d)** Bathymetry of the northeastern part of the study area. **(e)** Bathymetry of the eastern part of the study area showing irregularly shaped glacial lineations.

4.2 Sea floor landforms in Bessel Fjord

4.2.1 Large-scale geomorphology

Bessel Fjord contains a variety of basins that are separated by different styles of sills (Figs. 2, 5, and 6). The outermost sill is at the fjord's entrance, and it commonly ranges in depth from 50 to 200 m, with major sections reaching above (and near) the water surface as there are islands in the fjord entrance. Four large basins that are elongated in a west–east direction have been identified in Bessel Fjord (B1–B4). The deepest basin, basin 1 (B1), is the closest to the fjord entrance and is separated from basin 2 (B2) by a >215 m high sill (M1) that is steeper to the east (Figs. 2 and 5). Basin 3 progressively deepens westwards, with a maximum depth of 380 m. A ~ 70 to 160 m asymmetrical sill (M3; Figs. 2 and 5) that is steeper on its east side separates basin 3 from basin 4. Basin 4 is the shallowest basin (~ 280–300 m) and is adjacent to multiple smaller basins that are primarily at lower points of elevation. The fjord also contains smaller basins that are raised relative to the average seafloor depth (Fig. 6e). Features interpreted as bedrock mounds have also been identified in other sections of the fjord (Figs. 5 and 6). Along the

fjord sides, landforms from sediment reworking, including slide scars, channels, and gullies, have also been observed Fig. 6b.

4.2.2 Linear ridges oriented along the fjord axis – glacial lineations

Oriented along the fjord's axis (or at times slightly oblique to it), linear features have been identified in the inner and middle parts of the fjord, and there is a single lineation on the outer part of the fjord (Figs. 5 and 6). They range in size from 100 to 1000 m in length and ∼ 3 to 9 m in height, although some that are as high as 80 m have been identified in the inner fjord. Their morphologies vary throughout the fjord, and their length-to-width ratios range from 2 : 1 to 5 : 1. Most ridges slope towards the outer fjord, although some slope in the opposite direction or have an irregular or flat top. They appear both independently in connection with inferred bedrock highs and in clusters in flat lying areas of basin 3. These ridges have been interpreted as glacial lineations, and they are thus indicating the direction of former glacier flow.

4.2.3 Transverse ridges – moraines

Several transverse ridges have been identified in the inner and central portion of the fjord, oriented perpendicular to the fjord's axis (Figs. 2, 5 and 6). The ridges in the innermost position of the fjord tend to largely conform to the topography (i.e., between bedrock mounds, some of which are positioned mid-fjord (M4–6; Fig. 6b), and the fjord sidewalls) and are the threshold between sub-basins (Fig. 6). The width and length of ridges range from 150 to 600 and 120 to 500 m, respectively, where their heights are between < 5 to 58 m.

A particularly large asymmetrical transverse ridge that spans the width of the fjord is situated between basins 3 and 4 (M3; Figs. 2 and 6d). This ridge is ∼ 1.5 km in width and between 72 to 162 m in height. It contains a crescent shape in aerial view and is concave towards the mouth of the fjord. A large threshold with a 1.8 km width and a > 215 m height also separates basin 1 and 2 (M1; Figs. 2 and 5). This feature is ∼ 150 m shallower in the north and dips steeply into basin 1.

The transverse ridges have been interpreted as moraines, which would have formed during glacial stillstands or readvancements during the retreat of a grounded tidewater glacier margin. These moraines do not fill the width of the innermost fjord, which has also been seen in inner Nordfjord (part of the Kaiser Franz Josef Fjord system) by Olsen et al. (2022). While the large transverse ridge M3 is believed to be a moraine, it is considered more likely that M1 is a bedrock mound based on its morphology. The smaller transverse ridges are interpreted as recessional moraines. Smaller moraines have the potential to form at ice margins annually (Lyså and Vorren, 1997; Dowdeswell et al., 2016) and have been observed with a variety of sizes and morphologies on the NE Greenland shelf (e.g., Winkelmann et al., 2010).

4.2.4 Sinuous ridges – eskers

Sinuous ridges, oriented parallel or oblique to the fjord's axis, occur in basin 3 (Figs. 5, 6b, d and e). These features have widths and lengths of 50 to 120 and 350 to 800 m, respectively, and heights of 10 to 15 m. The most pronounced examples of these ridges have been observed east of the large recessional moraine that has been previously discussed (Fig. 6e).

These sinuous ridges have been interpreted as eskers. These landforms form from sediment infill of subglacial and englacial conduits and have been identified in other studies in Greenland (Huddart and Lister, 1981; Geirsdóttir et al., 2000; Winkelmann et al., 2010; Lane et al., 2015). They frequently form in the direction of former ice flow often form during terminal stages of glaciation, and they are therefore associated with moraines (Shreve, 1985). They vary in size depending on the glacial drainage pattern, as well as a number of other factors; however, eskers identified within Bessel Fjord appear smaller than those identified in studies in Canada, the UK, and the Kola Peninsula in Russia (Storrar et al., 2014).

4.2.5 Wavy transverse ridges – sediment waves

Adjacent to the two eskers in basin 3 are a series of wavy transverse ridges to the east of a large recessional moraine (Figs. 5, 6b and d). These features occupy an area of ∼ 500 by 1500 m and contain small ridges and flat areas that slope at an angle of 3 to 6° to the east. Each wave "crest" is ∼ 50 to 100 m apart, although some appear to begin only halfway through the width of the area, where others occupy the entire width (north to south). These waves are crosscut by a channel to the north (Fig. 6d). North of this channel similar features with a wavy morphology occur, although these are substantially smaller.

These wavy transverse ridges have been interpreted as sediment waves. Sediment waves found associated with deltaic and glaciofluvial deltaic systems have been associated with retrogressive slope failures, gravity-induced sediment creep and/or the migration of sediment waves upslope (Cartigny et al., 2011; Hill, 2012; Stacey and Hill, 2016). Alternatively, given the position of the smaller wavy transverse ridges to the ice cap on Ad. S. Jensen Land (Figs. 1 and 2) and the larger ridges to the large moraine to the west (Figs. 5 and 6), it is also possible that these ridges are sets of moraines. Recessional moraines have been identified in the vicinity of eskers in Spitsbergen fjords (Ottesen et al., 2008; Kempf et al., 2013), which may account for the smaller wavy transverse ridges. The larger wavy transverse ridge do also resemble thrust moraines identified by Forwick et al. (2010). Further work may be required in the evaluation of these features. For a full list of observed landforms, see Table 4.

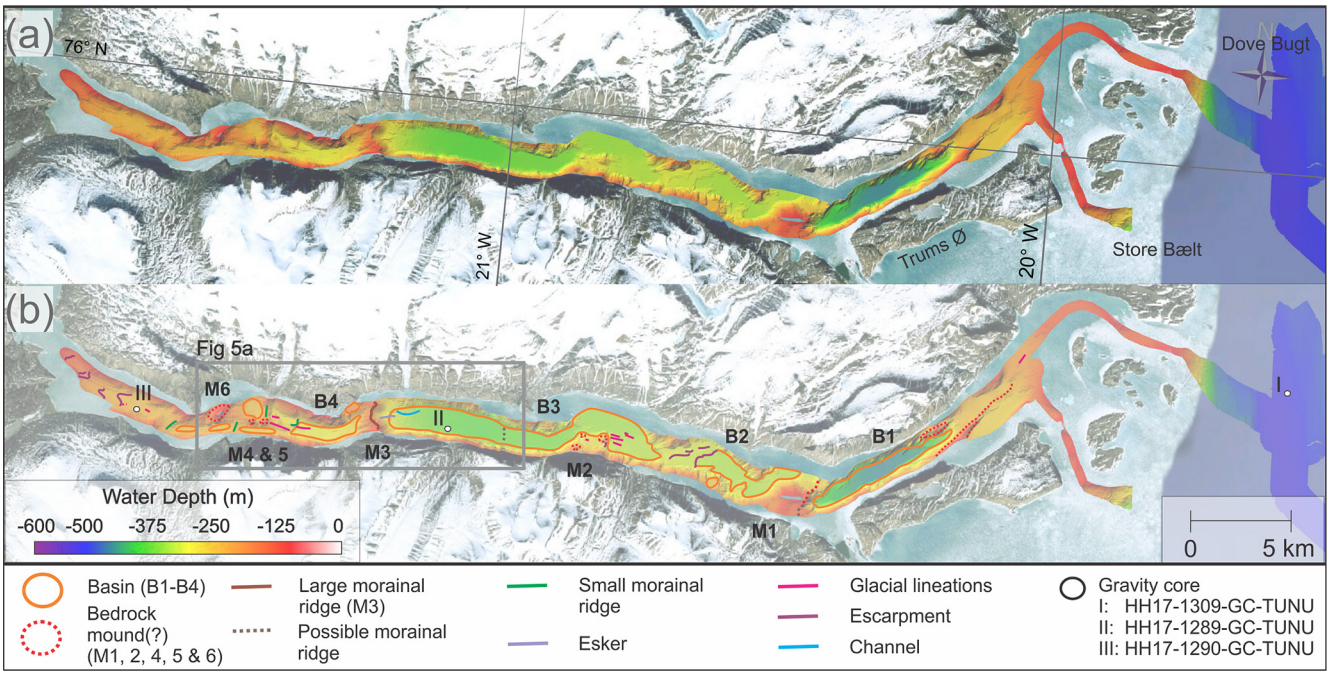

Figure 5. **(a)** Bathymetric map of Bessel Fjord. **(b)** A map of mapped features in Bessel Fjord. Satellite images obtained from Google Earth (© Google 2020).

Table 4. Overview of observed landforms in southern Dove Bugt and Bessel Fjord. [a] The "wide" features describe wide elongated ridges. [b] The "large ridge (M3)" feature is considered a transverse ridge.

Region	Description	Width	Length	Height	Notable feature	Interpretation
Dove Bugt	Elongated lineations	35–50 m	~ 1 – ≥ 10 km	< 1–3 m	Roughly N–S	Glacial lineations
	[a]Wide	200–650 m	3.8–8.8 km	4.5–15 m		
	Depression and mound	200 m	450 m	3–4 m	Mound to the south of the depression	Hill–hole pair
	Furrows (scour marks)	~ 40–100 m	< 100–200	3–5 m	Irregular	Iceberg plow marks
	Transverse ridges	150–400 m	~ 30–100 m	0.5–1 m	Roughly W–E	Recessional moraines
Bessel Fjord	Linear ridge	45–350 m	100–1000 m	3–9, 80 m	Parallel to the fjord's axis	Glacial lineations
	Transverse ridges	150–600 m	120–500 m	< 5–58 m	Perpendicular to the fjord's axis	Recessional moraines
	[b]Large ridge (M3)	1485 m	600–1600 m	72–162 m		Moraine
	Sinuous ridges	50–120 m	350–800 m	10–15 m		Esker
	Wavy transverse ridges	400–700 m	~ 45–100 m	2–5 m	Perpendicular to the fjord's axis	Sediment wave
	Elongated depression	~ 200 m	~ 1 km	6–8 m		Channels
	Chute	~ 20–100 m	60–400 m	1–15 m		Gullies

4.3 Lithostratigraphy

Three gravity cores were retrieved from the study area. Gravity core HH17-1309 was collected in Store Bælt and was sampled from a N-NW–S-SE-oriented depression that contains iceberg plowmarks and a MSGL. Gravity core HH17-1289 was collected in the middle of the Bessel Fjord and is located directly east of the above-mentioned sediment waves on the distal part of the pronounced transverse ridge. Nearby, a modern ice-cap-fed glaciofluvial channel is observed in satellite imagery, likely with a delta at its fjord termination. The gravity core HH17-1290 was collected within the inner fjord, west of the basins and thresholds observed in this study area and is the closest core to Soranerbræen (located ~ 9.7 km east of the glacier) (Fig. 7).

4.3.1 Facies

Facies 1 – laminated mud (Fl, Fl-d and Fl/m-d)

Facies 1 consists of laminated mud (Fl) and laminated mud with dropstones (Fl-d) and have been observed in all three gravity cores (Figs. 7, 8a, d and f). Laminations are composed of either mud or very fine sand. Mud laminations with finer laminations have also been identified in Unit 3.2 (100–200 cm; Fig. 7a, Fl/m-d). Microfractures have also been identified within this facies (Fig. 8f).

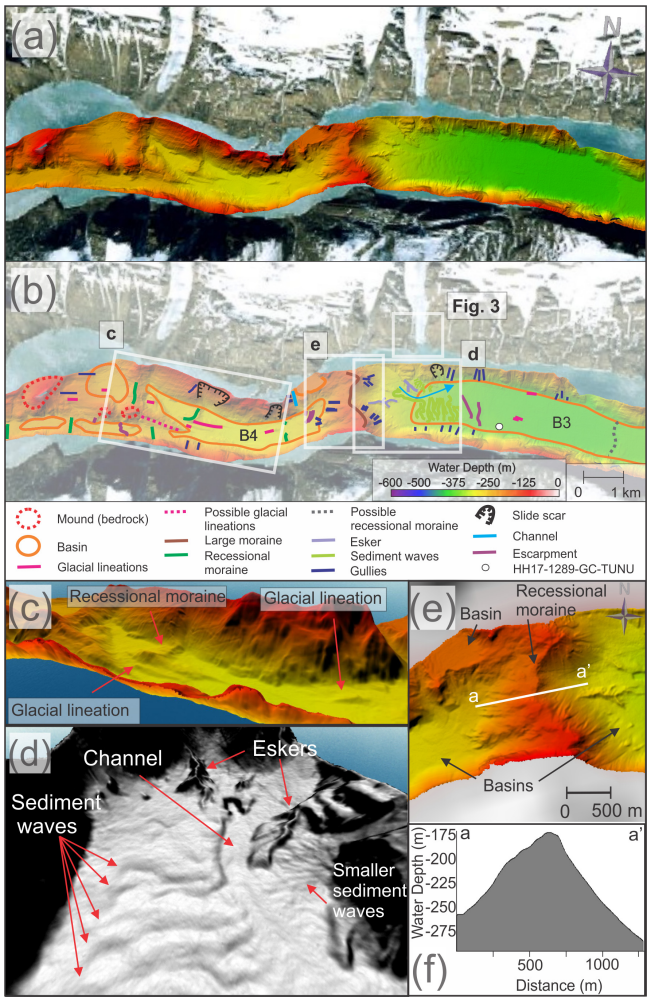

Figure 6. **(a–b)** Mapped sections from inner to middle Bessel Fjord. Background images used for **(a)** and **(b)** have been obtained from Google Earth (© Google 2020). **(c)** Glacial lineations in basin 4 (B4). **(d)** Eskers, sediment waves, and a channel in basin 3 (B3). **(e)** A large moraine (M3) between B3 and B4. Note the raised sub-basin to the west and esker to the east. **(f)** Profile across the large recession moraine (M3).

Wet bulk density measurements tend to increase with depth in some sections of this facies (e.g., 87–350 cm in HH17-1309), suggesting normal sediment consolidation. However, a stagnation or decrease in wet bulk density with depth in other sections (e.g., below ∼ 350 cm in HH17-1309) suggests less consolidation. The magnetic susceptibility generally tends to increase with depth in HH17-1309 and in Unit 3.2 in HH17-1290; however, the remainder of this facies in HH17-1290 (Unit 3.1) remains relatively stable to the base of the core. Notable positive peaks have been identified at 110 and 140 cm in HH17-1309, and measurement fluctuations occur in HH17-1289. Peaks in magnetic susceptibility may reflect the introduction of turbidites or clasts where fluctuations may reflect shifts in sediment provenance.

Muds with sand laminations are believed to have formed through a combination of ice-proximal suspension settling from overflow plumes and turbidity-current activity (underflows). The rhythmically laminated muds are believed to have formed from ice-proximal suspension settling from turbid overflow plumes. Similar laminated sediments have been identified in Kaiser Franz Joseph Fjord and Fosters Bugt in eastern Greenland and are theorized to have been deposited from turbid meltwater plumes in an ice-proximal environment (Evans et al., 2002). Large clasts have been interpreted as ice-rafted debris (IRD). The formation of microfractures may have been caused by soft sediment deformation, possibly from grounded icebergs.

Facies 2 – massive mud (Fm and Fm-d)

The second facies consists of massive mud with or without dropstones and can be found in the inner fjord core HH17-1290 and the Store Bælt core HH17-1309 (Fig. 7). In HH17-1290 this appears down core between sections of Facies 1 and in the topmost unit, Unit 3.3. The magnetic susceptibility gradually increases down core in this facies in Unit 3.3. Further down core, in Unit 3.2, this facies is associated with a downwards trend in magnetic susceptibility following peaks in measured readings. Wet bulk density values roughly mirror these trends. In HH17-1309 massive mud units have been observed in Unit 1.4, where magnetic susceptibility and wet bulk density values increase down core.

This facies is interpreted as being the result of suspension settling from overflow plumes and is believed to have been deposited in an ice-distal glaciomarine environment with varying input from IRD (i.e., Boulton and Deynoux, 1981). Sediment may be sourced from a single location (i.e., Soranerbræen) or more than one location (e.g., local ice caps) in an ice-distal glaciomarine environment with limited iceberg or sea ice rafting. Massive mud deposits have also been identified in other Greenland fjords (e.g., Ó Cofaigh et al., 2001), and it has been suggested that they may indicate meltwater from distal ice or fjord margin conditions (Evans et al., 2002).

Facies 3a – laminated sand (Sh)

Facies 3a consists of sections of sand with horizontal sand laminations. This facies has been predominantly observed in the mid-fjord core, HH17-1289-GC-TUNU (Figs. 7 and 8d). These sections consist of fine- to medium-grained sand that range in thickness and colors. Occasionally this facies also contains normal graded bedding (e.g., Fig. 8d, ∼ 174–183 cm). This facies does not contain uniform magnetic susceptibly or wet bulk density readings as it has been found in association with low and high peaks of both parameters and values that are near the average for the core.

This facies is interpreted as being deposited from turbidity currents, possibly underflows that are either sourced from

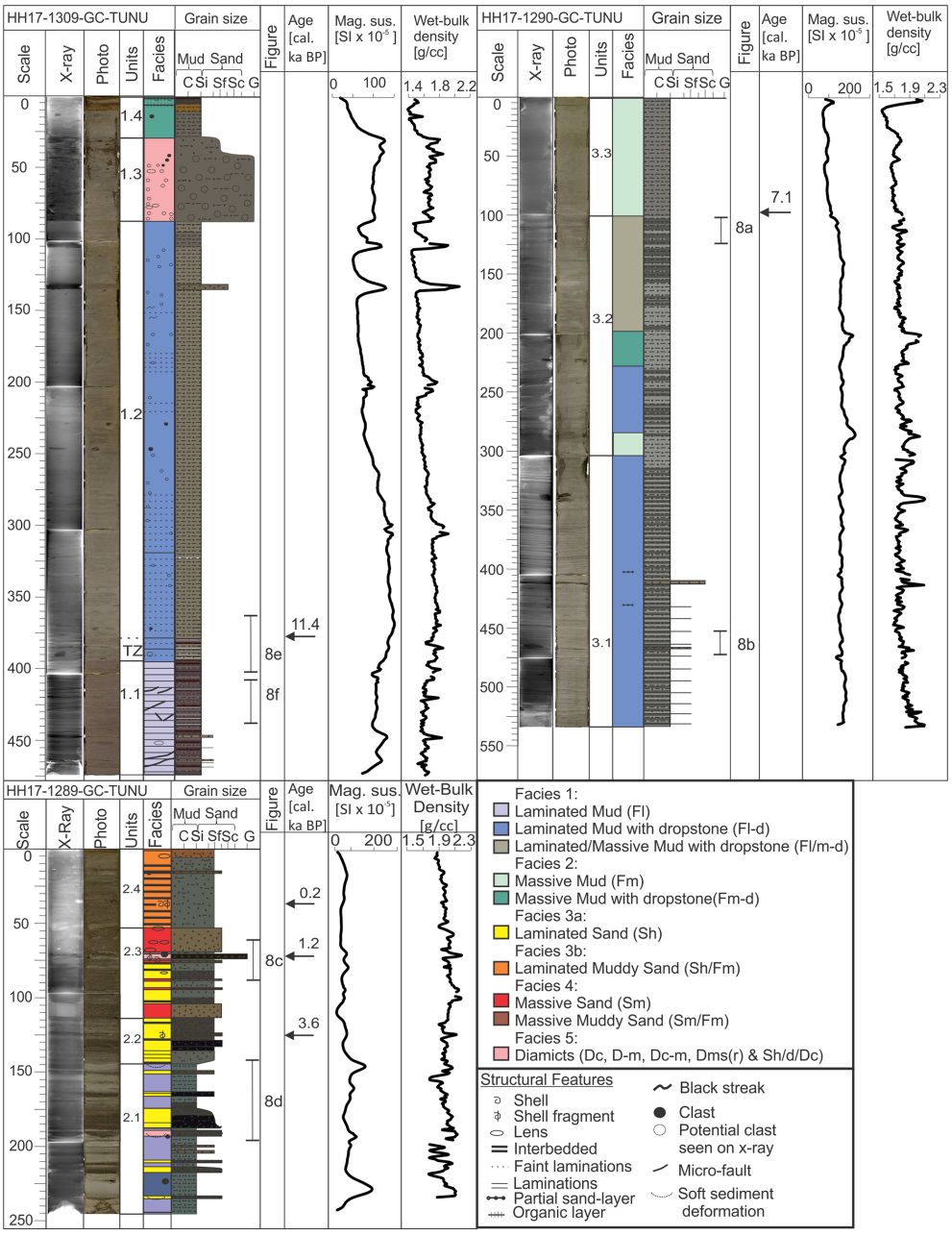

Figure 7. Lithological core logs of the three gravity cores with X-ray images, core photos, unit divisions, facies, structures, magnetic susceptibility, and wet bulk density. TZ in HH17-1309-GC-TUNU stands for "transition zone". Grain size abbreviations are as follows: C: clay; Si: silt; Sf: fine-grained sand; Sc: coarse-grained sand; and G: gravel.

glacial or non-glacial streams and slope failures. Uniform layers may indicate a single, rapid event, where shifts in grain size and color may be the result of short-lived fluctuations in sediment input. Laminated sands have been identified in Scoresby Sund in eastern Greenland and have also been attributed to turbidite formation (Ó Cofaigh et al., 2001).

Facies 3b – laminated muddy sand (Sh/Fm)

Facies 3b represents sections of sand with faint horizontal laminations and a large quantity of clay material interspersed throughout with faint laminations. This has been observed in HH17-1289 at the topmost unit in the core, Unit 2.4 (Fig. 7). Magnetic susceptibility is relatively uniform in this facies, where the wet bulk density tends to decrease up core. Sediment grain size analysis of a single sample from this facies

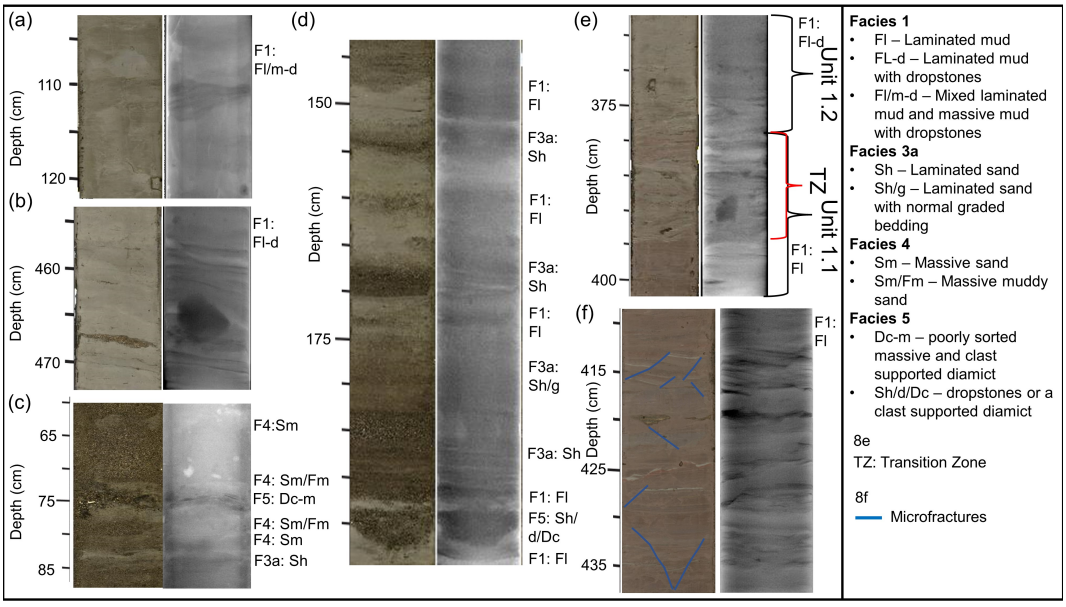

Figure 8. Photographic and X-ray images of sections of the three gravity cores **(a–f)**. Corresponding facies codes can be found to the right of each image.

revealed that the sediment is composed of 56.3 % sand and 43.7 % mud. A "patch" of black organic material (i.e., plant material and shells) was also identified within this unit.

This complex facies is believed to have formed predominantly from underflow events, sandy and muddy turbidites, or alternatively sandy turbidites with additional input from suspension settling. Similar deposits have been observed in Balsfjord, Norway, albeit without lamination and possibly a higher mud content (Forwick and Vorren, 1998).

Facies 4 – massive sand and massive muddy sand (Sm and Sm/Fm)

Facies 4 contains sections of massive sand (Sm) and massive sand with a large amount of clay content (Sm/Fm). This facies is predominantly found in Unit 2.3 (and to a much lower extent, Unit 2.4) in HH17-1289 (Fig. 7). Sections of massive sand have been found in association with mud lenses and often contain horizontal sand layers (Sh) above and below it. Slight increases and decreases in magnetic susceptibility values have been observed within this facies.

This facies is believed to have developed through rapid deposition and deformation of Facies 3a and b. According to this interpretation, the mud lenses observed in this facies were once layers or lamina that became deformed due to the sand–mud density contrast. Massive sand has been found in Kangerlussuaq and Miki fjords in eastern Greenland (Smith and Andrews, 2000), and well-sorted coarse-grained deposits have been recovered near Petermann Glacier in northern Greenland (Reilly et al., 2019). Authors have attributed these layers to sediment gravity flows.

Facies 5 – diamicts (Dc, D-m, Dc-m, Dms(r), and Sh/d/Dc)

Facies 6 contains a variety of different diamicts observed within the mid-fjord core HH17-1289 and the Store Bælt core HH17-1309. In HH17-1289 this includes a 3.5 cm poorly sorted, massive, and clast-supported diamict (Dc-m) in the middle of Unit 2.3 (Figs. 7 and 8c) and a horizontally laminated layer of sand that is either accompanied by dropstones or a clast-supported diamict (Sh/d/Dc) (Figs. 7 and 8d). It is inferred that they are the result of sea ice or iceberg rafting or dumping. Within HH17-1309 there is a substantially larger, sharp-based, matrix-supported diamict that is stratified in its upper part (Dms(r)) in Unit 1.3 (Fig. 7). Based on these characteristics, this diamict has been interpreted as a density flow deposit, likely a debris flow deposit that is overlain by (part of) a turbidite.

4.3.2 Core chronology

Shell and shell fragments were recovered from HH17-1289 for radiocarbon dating. At 34 cm depth, a semi-spherical path of organic content was identified, containing two intact *Yoldiella lenticula*, a shell fragment, and plant material. Additionally, at 71 cm depth, a large 3 cm half of a *Hiatella arctica* shell was collected for dating, and shell fragments were recovered from a depth of 125 cm for the same purpose. These shells yielded radiocarbon ages of 0.2, 1.2, and 3.6 cal ka BP, respectively (Table 5).

Cores HH17-1290 and HH17-1309 were subsampled for foraminifera material at four positions, and calcareous benthic species were used for dating. In HH17-1290

Table 5. Calibrated radiocarbon dates.

Coring station	Sampling depth [cm]	Lab no.	Species	^{14}C age BP	Marine20 cal BP (1σ range)	Marine20 cal BP
HH17-1309-GC-TUNU	377	5157.1.1	Mixed benthic foraminifera	10357 ± 95	11 201–11 553	11 386
HH17-1289-GC-TUNU	35	5154.1.1	*Yoldiella lenticula*	688 ± 34	61–253	158
HH17-1289-GC-TUNU	71	5155.1.1	*Hiatella arctica*	1747 ± 28	1065–1250	1152
HH17-1289-GC-TUNU	125.5	5156.1.1	Bivalve frag.	3809 ± 36	3472–3701	3596
HH17-1290-GC-TUNU	97	5158.1.1	Mixed benthic foraminifera	6800 ± 80	6990–7250	7116

this included predominantly *Melonis barleeanus* and small amounts of *Islandiella norcrossi*. In HH17-1309, at a depth of 377 cm *Islandiella norcrossi* (rare to common), *Stainforthia feylingi* (rare), and a planktonic species were identified immediately above the transition zone between two facies. Radiocarbon dates for the HH17-1309 sample yielded an age of 11.4 cal ka BP, where the sample from HH17-1290 yielded an age of 7.1 cal ka BP (Table 5).

5 Discussion

5.1 Ice sheet advance

The appearance of glacial lineations in Bessel Fjord suggest that the fjord was once fully glaciated, which is in accordance with the inferred shelf break-terminating ice sheet inferred for the LGM from other studies (e.g., Laberg et al., 2017; Olsen et al., 2020) (Fig. 9a and b). Ice that filled the fjord is believed to most likely be from the modern Soranerbræen glacier but may have also included ice caps and other nearby branches of inland ice.

Glacial lineations are believed to have formed during the LGM but could have also formed during an ice readvance in the deglaciation (see below). Onshore and south of Bessel Fjord, two sets of striations identified in Langsødalen (Hjort, 1979, 1981) may suggest that this valley experienced two glaciation events (Fig. 1c). Striations and lateral moraines found along the fjord axis may be the result of the east–west movement of ice through the valley, where SW-oriented striations may be the result of Storstrømmen encroaching also onto terrestrial areas. Hjort (1981) suggested that striae on Haystack may indicate that ice flow was dominant from the north during the Nanok Stadial but ice pressure from Langsødalen dominated later after deglaciation begun. Thus, it is possible that ice masses drained through both Bessel Fjord and Langsødalen during full glacial conditions further advancing into Dove Bugt and Store Bælt.

In Store Bælt, the orientation of glacial lineations (e.g., MSGLs) suggest that ice flowed to the south along the west cost of Store Koldewey, marking the southwards expansion of the Storstrømmen ice stream (Fig. 9a and b). East of Dove Bugt, MSGLs identified in Store Koldewey Trough are believed to have formed when the Storstrømmen ice stream acted as a "pure" ice stream (Bentley, 1987; Stokes and Clark, 1999) and overrode the underlying topography during the LGM (Fig. 9a; Olsen et al., 2020). It was theorized that at a later phase, when the ice sheet began to thin, the ice stream became more influenced by the topography of deep troughs, draining northwards to Jøkelbugten and southwards to Dove Bugt (Olsen et al., 2020). Assuming these two phases occurred in the Storstrømmen ice stream development, it is possible that these glacial lineations in Store Bælt represent a period when a branch of the ice stream began conforming to topographical controls (e.g., Store Koldewey) and flowed towards the south. At this point the ice may have flowed into the southeast through Dove Bugt Trough (Fig. 9a).

An alternative interpretation that cannot be excluded is that these MSGLs formed during a glacial re-advance that followed the LGM. Between Hochstetter Forland and Shannon Ø a submerged moraine has been identified in Shannon Sound, which may indicate that at one point the ice stream traveled south rather than through Dove Bugt Trough (Figs. 9b and 10a; Hjort, 1981; Landvik, 1994; Larsen et al., 2016; Funder et al., 2021). However, constraints from Store Koldewey, Germania Land, and Trums Ø do not support an ice advance during the Younger Dryas (Fig. 10b; see below). The formation of the submerged moraine was possibly due to an ice readvance of the GrIS outlet(s) (Soranerbræen, L. Bistrup Bræ and/or Storstrømmen) through the western inner Dove Bugt (Fig. 9b), where the surroundings (onshore and offshore) were not affected or less affected. If this is correct, the readvance may have occurred during the Younger Dryas (prior to 11.4 cal ka BP; see below).

5.2 Ice sheet retreat through Store Bælt

The deglaciation age of 11.4 cal ka BP (Table 5) from Store Bælt immediately east of the Bessel Fjord entrance is attributed to the retreat of a N–S-bound branch of the NEGIS (Fig. 9c) due to the presence of N–S-oriented glacial lineations near the gravity core. This date represents a minimum age for the deglaciation as it is not from the base of the deglacial deposits. Previously published dates constraining the timing of deglaciation in Dove Bugt have been restricted to terrestrial regions (Fig. 10b). Using cosmogenic nuclide dating, Skov et al. (2020) produced deglaciation ages of ca. 12.7 ka at Store Koldewey and ca. 9.8 ka at Pusterdal, and later Larsen et al. (2022) produced a number of deglacia-

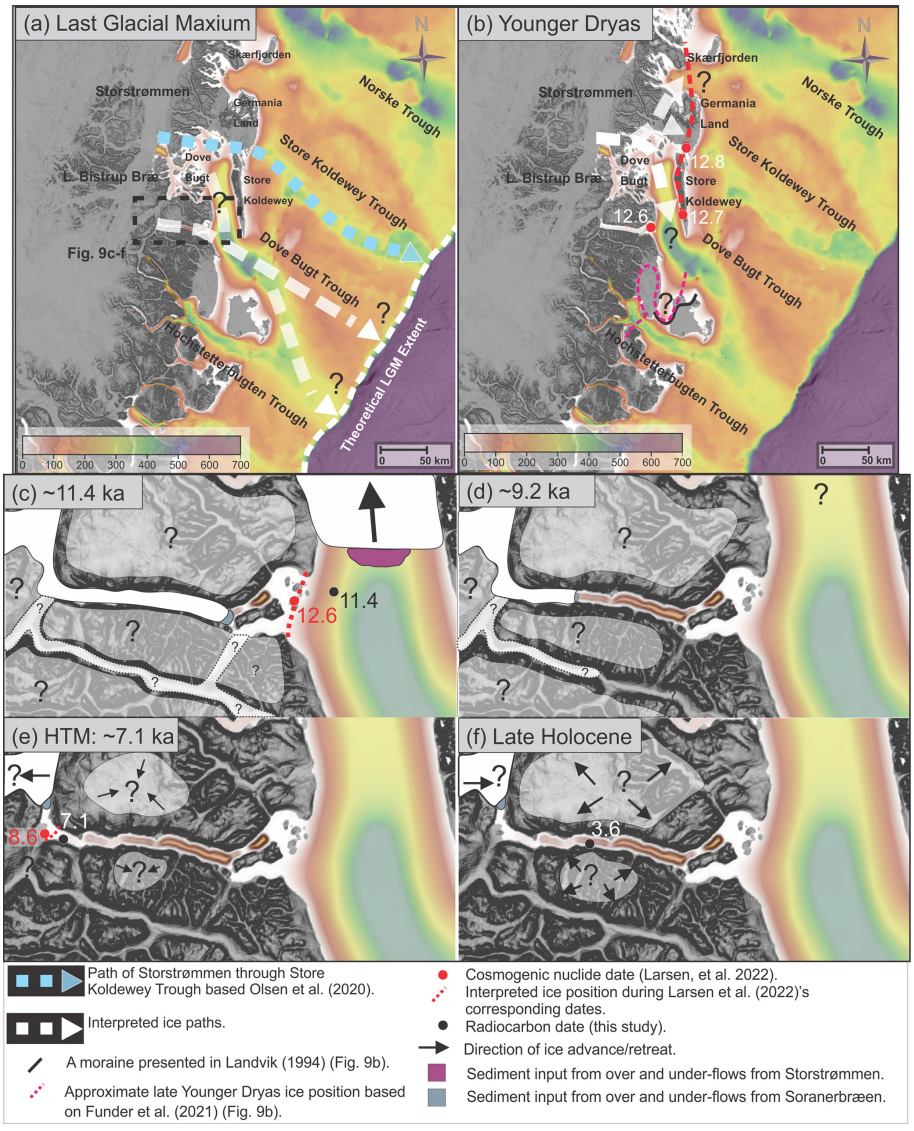

Figure 9. Maps showing ice sheet extent and advancement or retreat directions in SW Dove Bugt and Bessel Fjord during a range of periods. **(a)** The interpreted position of the ice sheet during the LGM. **(b)** The theoretical position of ice in Bessel Fjord and Dove Bugt during the Younger Dryas. **(c)** The ice position in Bessel Fjord at ∼ 11.4 ka based on approximated deglaciation date presented in this study and the position and radiocarbon date for gravity core HH17-1309. The size of ice caps in **(c)**–**(f)** are only indicative. **(d)** The position of ice in Bessel Fjord at ∼ 9.2 ka based on approximated deglaciation data from this study. **(e)** Ice retreating beyond our gravity core (HH17-1290) at ∼ 7.1 ka during the HTM. **(f)** The Late Holocene ice expanse in Bessel Fjord with a radiocarbon date from gravity core HH17-1289. Background bathymetry displayed using IBCAO data (Jakobsson et al., 2020).

tion ages across Dove Bugt and Bessel Fjord (8.6–12.8 ka) (Fig. 10b).

Our minimum age of ∼ 11.4 cal ka BP from HH17-1309 largely matches findings in Dove Bugt and Hochstetter Forland (Fig. 10b). It is slightly later than average cosmogenic nuclide ages obtained from Larsen et al. (2022) on Trums Ø (12.6 ka) and a Nanok moraine on southern Store Koldewey (12.7 ka), but earlier than a second Store Koldewey Nanok moraine (11.0 ka) and positions closer to the modern ice margin of Storstrømmen, such as Licht Ø (10.8 ka) and Bræ Øerne (8.9 ka). Thus, Store Koldewey and Trums Ø may have been partially deglaciated slightly prior to the final retreat of the NEGIS through Store Bælt.

Radiocarbon dates obtained from lake sediments on Store Koldewey suggest that the earliest onset of warmth may have begun ∼ 10 cal ka BP (Klug et al., 2009b); therefore, the deglaciation of the area beginning prior to this may further support these results. Additionally, Landvik (1994) produced a range of deglaciation ages between 9.6 to 8.5 cal ka BP along the northern coast of Dove Bugt (Hvalrosodden and

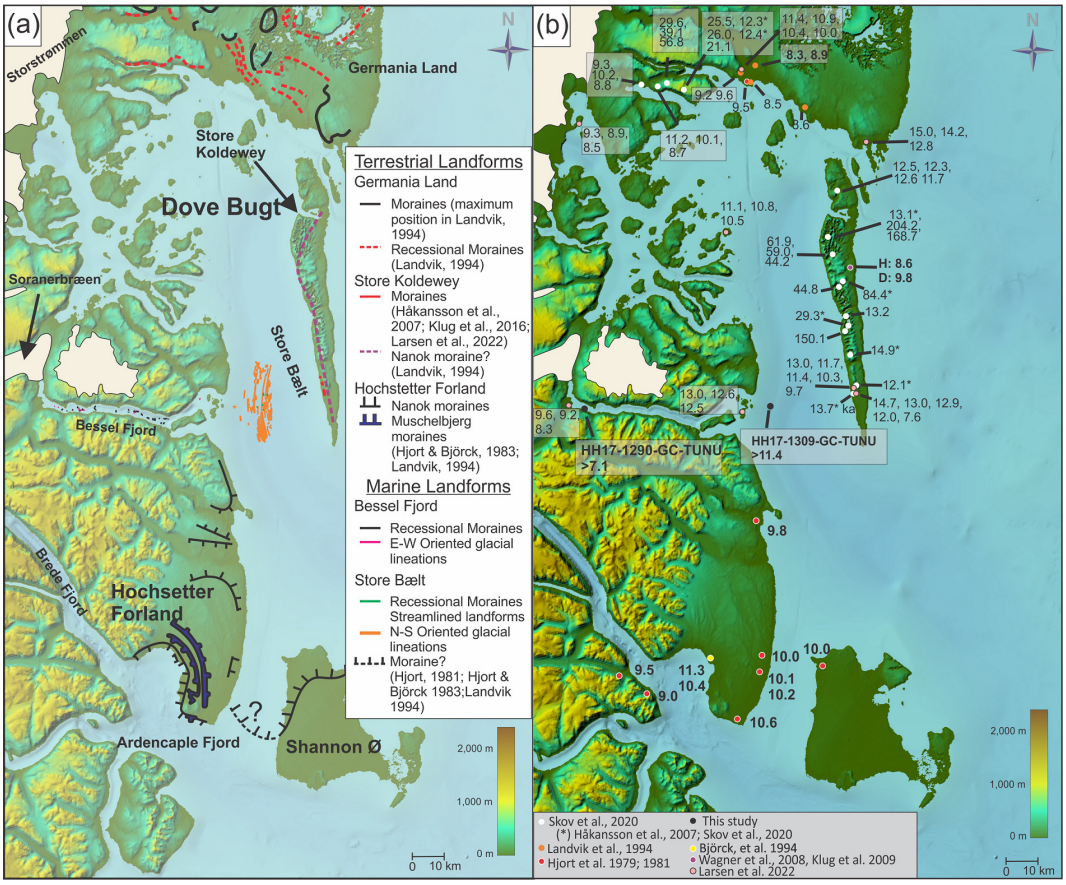

Figure 10. **(a)** Marine moraine ridges and glacial lineations from the current study together with previously mapped marine and terrestrial features. **(b)** Location of deglaciation dates from this study (Table 5) and previous publications. See Table 3 for recalibrated radiocarbon dates. H is Hjort Lake, and D is Duck Lake. The background displayed uses IBCAO data (Jakobsson et al., 2020).

Snenæs on Germania Land) and Hjort (1981, 1979) provided a range of delegation ages between 10.6 to 9.8 cal ka BP on Hochstetter Forland. Later, Björck et al. (1994), on Hochstetter Forland, dated *Hiatella arctica* shells near the shore of Peters Bugt Sø and *Portlandia arctica* shells in a delta distal to a Nanok I ridge to 10.4 and 11.3 cal ka BP, respectively (Table 3; Fig. 10b).

Although based on a limited dataset, the lack of prominent morainic landforms in Store Bælt may also suggest a rapid retreat through the region. A small number of retreat moraines have been observed in an isolated region of the study area, but the most prominent geomorphic landforms are glacial lineations. Placing Store Bælt within the context of Dowdeswell et al. (2008)'s proposed model for ice streams in high latitudes, ice likely retreated through the area rapidly, although the presence of small moraines may suggest brief periods of stagnation. This is in accordance with findings by Larsen et al. (2020, 2022) that deep fjords and outer regions in eastern northern Greenland were rapidly deglaciated between ∼ 12.6 and 10 ka. However, additional data are required to confirm this.

Oceanic warming is believed to have contributed to the deglaciation of the inner shelf further north and south of Dove Bugt (e.g., Jackson et al., 2022; Davies et al., 2022). Within the study area, Store Koldewey does largely block oceanic water from the shelf from entering Store Bælt; however, it is possible that warmer water traveled through the Dove Bugt Trough to the south and impacted a north–south branch of the ice stream. This mechanism for warm water transport has also been suggested for other eastern Greenland troughs (Arndt et al., 2015) and used to explain how warm water has reached other outlets of the NEGIS (e.g., Zachariae Isstrøm via the Norske Trough (Schaffer et al., 2017)).

5.3 Ice sheet retreat through Bessel Fjord

Cosmogenic nuclide dates from Trums Ø suggest that the deglaciation of the outer fjord began around 12.6 ka (Larsen et al., 2022). Gravity core HH17-1290, collected from the inner fjord region, consists of sediments that reflect an increasingly ice distal environment up core. One radiocarbon date from the core provides a minimum age of ∼ 7.1 cal ka BP for the deglaciation of Soranerbræen and/or local ice caps from

the inner fjord region (Table 5 and Fig. 9e). This date, however, is not from the base of the deglacial deposits and therefore represents a minimum age for the deglaciation of the inner fjord. New cosmogenic nuclide dates from Vandrepasset (onshore the innermost Bessel Fjord area, connecting the fjord and the next valley to the south) provide an age of 8.6 ka for the deglaciation of the innermost fjord area (Larsen et al., 2022), confirming this interpretation. Our minimum age of 7.1 cal ka BP and the results of Larsen et al. (2022) fall within a modeled ice sheet extent by Lecavalier et al. (2014), which placed the position of the ice sheet in the middle of Bessel Fjord at 9 cal ka BP, and the present-day ice margin is reached by 6 cal ka BP. The minimum age also agrees with the onset of HTM on Store Koldewey (∼ 8.0 to 4.0 cal ka BP) (Wagner et al., 2008; Klug et al., 2009a; Schmidt et al., 2011) and Hochstetter Forland (8.8 and 5.6 cal ka BP) (Björck and Persson, 1981; Björck et al., 1994). Thus, the GrIS retreated from the marine realm in Early Holocene, slightly before or at the time of the HTM in this region (characterized by a mean July temperature 2–3 °C higher than at present; Bennike et al., 2008).

The appearance of recessional moraines in Bessel Fjord suggests that the fjord underwent a stepwise deglaciation. The large moraine identified between Basin 3 and Basin 4 (M3; Fig. 7e) is believed to have formed during a major ice halt or readvance and was possibly climatically induced. Smaller moraines occasionally follow topographic boundaries, which may suggest that the retreat of ice in Bessel Fjord was also partly topographically controlled. Recessional moraines identified by Olsen et al. (2020) east of Dove Bugt in Store Koldewey Trough contain similar heights to those identified here (excluding M3). However, there are more moraines identified in Store Koldwey Trough than in Bessel Fjord, and they are wider, which is likely due to the lack of topographic confinement.

A decrease in atmospheric temperatures in Early Holocene is recorded in the Greenland Summit temperature records and includes the Preboreal Oscillation and the 9.2 ka event (Kobashi et al., 2017). We tentatively suggest that some of the moraines identified in the Bessel Fjord may have developed during some of these events. From this we suggest that increased Northern Hemisphere summer insolation that peaked in the Early Holocene was the main control for this part of the deglaciation during which the ice front receded from the coastline to the west of (onshore) Bessel Fjord, a distance of ∼ 60 km. Assuming that this occurred over a maximum period of ∼ 4.3 cal ka BP (11.4–7.1 cal ka BP; see discussion above on the timing and length of this period), this corresponds to an average minimum ice recession rate of ∼ 14 m yr^{-1}. Further supporting this average rate, if one applies this same approach to the two average Bessel Fjord cosmogenic nuclide dates presented by Larsen et al. (2022) (12.6–8.6 ka) and the distance between their sampling locations (∼ 56 km), it also results in a rate of 14 m yr^{-1}. This rate is considered realistic as it is half (or less) than the rate estimated from the Nioghalvfjerdsfjorden further north (also part of the Storstrømmen ice stream), where a rate of ∼ 30–40 m yr^{-1} was reported (Bennike and Björck, 2002). This rate places Soranerbræen near the large moraine M3 around the 9.2 ka event (Fig. 9d).

While oceanic warming may be partially responsible for the retreat of the NEGIS through Store Bælt, we believe that Bessel Fjord is too sheltered by the sill at its entrance to have allowed warm, intermediate water to enter and make a significant impact of the deglaciation of the southern outlet of Soranerbræen. Our bathymetric dataset reveals that the depth of the sill is between ∼ 50 to 200 m; however, large parts of it are above water and form islands. This is far shallower than other fjord sills in the region that are theorized to have blocked warm Atlantic Water (e.g., the sill in Dijmphna Sund to the north, which has a maximum depth of 170 m; Wilson and Straneo, 2015). Also, the effect of the glacio-eustatic readjustment is considered to be small for this region, and was ∼ 9.5 m higher in the Young Sound region (slightly south of our study area) 7500 years ago (Pedersen et al., 2011). Rignot et al. (2022) also theorized that seafloor topography may impact whether warm water is reaching the northern outlet of Soranerbræen. They suggested further that the grounding line retreat of Storstrømmen, L. Bistrup Bræ, and possibly Soranerbræen may be primarily caused by ice thinning from atmospheric warming (Rignot et al., 2022). We suggest that a similar mechanism may be responsible for Soranerbræen's retreat through Bessel Fjord during the deglaciation.

5.4 Holocene glacier variability and sedimentary processes in Dove Bugt

Sedimentological evidence (e.g., ice-proximal laminated muds) from HH17-1309 suggests that suspension settling from a glacial source(s) likely dominated southwestern Dove Bugt during the Holocene. The contribution of sediment from the NEGIS seems unlikely, as Pusterdal became deglaciated by 9.5 ka (Skov et al., 2020) and Storstrømmen retreated beyond Bræ Øerne by 8.9 ka (Larsen et al., 2022); therefore, it may very well be from Soranerbræen or local ice caps.

During the latter part of the HTM in the middle Holocene, a time period in which some glaciers are believed to have reached their minimum extent across Greenland, the NEGIS is believed to have retreated beyond its current position between 5.4 and 1.2 cal ka BP (Table 3), creating the Storstrømmen Sound (Weidick et al., 1994). Laminations appear less frequently in the upper part of core HH17-1309, but they are not absent. Laminations are entirely absent in the Bessel Fjord core HH17-1290 during this period and remain absent through the colder Late Holocene. Later, during the Little Ice Age, Storstrømmen has demonstrated to have expanded to its modern day position (Weidick et al., 1994).

Gravity core HH17-1289, collected to the north of an onshore glaciofluvial channel connected to a modern-day ice

cap, transitions to complex assortment of sand layers just prior to 3.6 cal ka BP (Fig. 7). Sedimentological evidence suggests that these sand layers are largely the result of rapid, short-lived depositional events (i.e., turbidity currents) interpreted to be related to the growth of a delta slightly south of the core site, from glaciofluvial sediment input from a nearby outlet glacier.

Pollen assemblage data from Hochstetter Forland mark the end of the HTM at 5.6 cal ka BP (Björck and Persson, 1981; Björck et al., 1994), and information derived from aquatic organisms mark the end of the HTM on Store Koldewey at 4 cal ka BP (Wagner et al., 2008; Klug et al., 2009b; Schmidt et al., 2011). This coincides with the onset of turbidites in core HH17-1289. Therefore, it is possible that this shift to sand-dominated sedimentation within this core was controlled by climatically driven processes. This onset is here suggested to result from higher sediment input through the channel as local ice caps expanded outwards following the HTM, possibly in response to this climate cooling (Fig. 9f). This period of cooling also corresponds to extended concentrations of sea ice on the shelf (Kolling et al., 2017).

6 Conclusion

- Glacial lineations (MSGLs) identified in SW Dove Bugt suggest fast-flowing ice, interpreted to be from the NEGIS, developed during the LGM or an ice readvance during the deglaciation.

- Our minimum deglaciation date for Store Bælt (> 11.4 cal ka BP) is slightly younger than new cosmogenic nuclide dates found onshore on Trums Ø and one of two Nanok stadials on Store Koldewey (Larsen et al., 2022), as well as various other dates across Store Koldewey (e.g., Skov et al., 2020). Thus, Store Koldewey and Trums Ø may have been partially deglaciated prior to the final retreat of the NEGIS through Store Bælt.

- Moraines in Bessel Fjord (to the west of Dove Bugt) suggests that the fjord underwent multiple halts/or readvances upon deglaciation. Thus, the bathymetry of Bessel Fjord indicates that the glacial dynamics of the fjord were more dynamic than onshore evidence suggests.

- The radiocarbon date of 7.1 cal ka BP obtained in an inner fjord core is interpreted as a minimum age at which Soranerbræen retreated to or beyond its present-day onshore position west of the fjord and is in conformity with cosmogenic nuclide dates presented by Larsen et al. (2022) in the onshore inner fjord (8.6 ka).

- An average ice recession rate in Bessel Fjord was determined to be $\sim 14\,\mathrm{m\,yr^{-1}}$ using data from this study as well as cosmogenic nuclide dates from Larsen et al. (2022).

- The GrIS retreated from the marine realm in the Early Holocene, around the time of the onset of the HTM in this region. From this we suggest that increased Northern Hemisphere summer insolation that peaked in the Early Holocene was the main control for this part of the deglaciation.

- Sedimentological evidence after 7.1 cal ka BP in HH17-1289 (i.e., the presence of only massive mud) suggests that Soranerbræen did not expand back into Bessel Fjord for the remainder of the Holocene.

- The transition of mud to muddy sand at 4 cal ka BP in a mid-fjord core HH17-1289 may provide evidence for local ice cap growth. Thus, ice caps in Bessel Fjord may have fluctuated with greater sensitivity to climatic conditions than the NE sector of the GrIS during the cooling phase that followed the HTM.

Data availability. Bathymetry and Multi Sensor Core Logger (MSCL) data has been made available at UiT's open research data repository. Please see Zoller et al. (2022, https://doi.org/10.18710/IXW3VA).

Author contributions. JSL and TAR designed this study and collected the new data during the 2017 TUNU VII cruise. The bathymetrical and lithological data were interpreted by KZ in collaboration with JSL and TAR. KZ prepared the manuscript with contributions from all co-authors.

Competing interests. The contact author has declared that none of the authors has any competing interests.

Disclaimer. Publisher's note: Copernicus Publications remains neutral with regard to jurisdictional claims in published maps and institutional affiliations.

Acknowledgements. We would like to thank the participants of the 2017 TUNU cruise to Greenland for making this project possible. A special thanks to the captain and crew of the RV *Helmer Hanssen* for their involvement in the cruise and assistance in collecting the data. Thanks also go out to the lab staff at UiT, Trine Dahl, Karina Monsen, and Ingvild Hald, who assisted with processing sediment core samples for this project. We would also like to thank Gesine Mollenhauer and the lab staff at the Alfred Wegener Institute for providing us with radiocarbon dated material using their MICADAS. Funding for this work was provided by UiT The Arctic University of Norway. Finally, we would like to thank the editor Marit-Solveig Seidenkrantz and our two reviewers for their constructive and helpful comments that ultimately improved the manuscript.

Financial support. This research has been supported by the Universitetet i Tromsø.

Review statement. This paper was edited by Marit-Solveig Seidenkrantz and reviewed by two anonymous referees.

References

Arndt, J. E.: Marine geomorphological record of Ice Sheet development in East Greenland since the Last Glacial Maximum, J. Quaternary Sci., 33, 853–864, https://doi.org/10.1002/jqs.3065, 2018.

Arndt, J. E., Jokat, W., Dorschel, B., Mykleburst, R., Dowdeswell, J. A., and Evans, J.: A new bathymetry of the Northeast Greenland continental shelf: Constraints on glacial and other processes, AGU Publ. Geochem. Geophy. Geosy., 16, 267–300, https://doi.org/10.1002/2014GC005684, 2015.

Arndt, J. E., Jokat, W., and Dorschel, B.: The last glaciation and deglaciation of the Northeast Greenland continental shelf revealed by hydro-acoustic data, Quaternary Sci. Rev., 160, 45–56, 2017.

Batchelor, C. L., Dowdeswell, J. A., and Rignot, E.: Submarine landforms reveal varying rates and styles of deglaciation in North-West Greenland fjords, Mar. Geol., 402, 60–80, https://doi.org/10.1016/j.margeo.2017.08.003, 2018.

Bennike, O. and Björck, S.: Chronology of the last recession of the Greenland Ice Sheet, J. Quaternary Sci., 17, 211–219, https://doi.org/10.1002/jqs.670, 2002.

Bennike, O. and Weidick, A.: Late Quaternary history around Nioghalvfjerdsfjorden and Jøokelbugten, North-East Greenland, Boreas, 30, 205–227, https://doi.org/10.1111/j.1502-3885.2001.tb01223.x, 2001.

Bennike, O., Sørensen, M., Fredskild, B., Jacobsen, B. H., BöCher, J., Amsinck, S. L., Jeppesen, E., Andreasen, C., Christiansen, H. H., and Humlum, O.: Late Quaternary Environmental and Cultural Changes in the Wollaston Forland Region, Northeast Greenland, Adv. Ecol. Res., 40, 45–79, https://doi.org/10.1016/S0065-2504(07)00003-7, 2008.

Bentley, C. R.: Antarctic ice streams: a review, Geophys. Res., 92, 8843–8858, 1987.

Biette, M., Jomelli, V., Chenet, M., Braucher, R., Rinterknecht, V., and Lane, T.: Mountain glacier fluctuations during the Lateglacial and Holocene on Clavering Island (northeastern Greenland) from ^{10}Be moraine dating, Boreas, 49, 873–885, https://doi.org/10.1111/bor.12460, 2020.

Björck, S. and Persson, T.: Late Weichselian and Flandrian biostratigraphy and chronology from hochstetter forland, northeast Greenland, Medd. Om. Grønl. Geosci., 5, 1–19, 1981.

Björck, S., Wohlfarth, B., Bennike, O., Hjort, C., and Persson, T.: Revision of the early Holocene lake sediment based chronology and event stratigraphy on Hochstetter Forland, NE Greenland, Boreas, 23, 513–523, https://doi.org/10.1111/j.1502-3885.1994.tb00619.x, 1994.

Boulton, G. S. and Deynoux, M.: Sedimentation in glacial environments and the identification of tills and tillites in ancient sedimentary sequences, Precambrian Res., 15, 397–422, https://doi.org/10.1016/0301-9268(81)90059-0, 1981.

Briner, J. P., McKay, N. P., Axford, Y., Bennike, O., Bradley, R. S., de Vernal, A., Fisher, D., Francus, P., Fréchette, B., Gajewski, K., Jennings, A., Kaufman, D. S., Miller, G., Rouston, C., and Wagner, B.: Holocene climate change in Arctic Canada and Greenland, Quaternary Sci. Rev., 147, 340–364, https://doi.org/10.1016/j.quascirev.2016.02.010, 2016.

Cartigny, M. J. B., Postma, G., Berg, J. H., and Mastbergen, D. R.: A comparative study of sediment waves and cyclic steps based on geometries, internal structures and numerical modeling, Mar. Geol., 280, 40–56, 2011.

Christiansen, J. S.: The TUNU-Programme: Euro-Arctic Marine Fishes – Diversity and Adaptation, in: Adaptation and Evolution in Marine Environments, 1, 35–50, https://doi.org/10.1007/978-3-642-27352-0, 2012.

Clark, C. D. and Stokes, C. R.: Palaeo-ice stream landsystem, in: Glacial Landscapes, edited by: Evans, D. J. A., Edward Arnold, London, 204–227, ISBN 0 340 80665 6, 2003.

Clark, C. D., Tulaczyk, S. M., Stokes, C. R., and Canals, M.: A groove-ploughing theory for the production of mega-scale glacial lineations, and implications for ice-stream mechanics, J. Glaciol., 49, 240–256, https://doi.org/10.3189/172756503781830719, 2003.

Cohen, J., Screen, J. A., Furtado, J. C., Barlow, M., Whittleston, D., Coumou, D., Francis, J., Dethloff, K., Entekhabi, D., Overland, J., and Jones, J.: Recent Arctic amplification and extreme mid-latitude weather, Nat. Publ. Gr., 7, 627–637, https://doi.org/10.1038/ngeo2234, 2014.

Cremer, H., Bennike, O., and Wagner, B.: Lake sediment evidence for the last deglaciation of eastern Greenland, Quaternary Sci. Rev., 27, 312–319, https://doi.org/10.1016/j.quascirev.2007.09.004, 2008.

Davies, J., Mathiasen, A. M., Kristiansen, K., Hansen, K. E., Wacker, L., Alstrup, A. K. O., Munk, O. L., Pearce, C., and Seidenkrantz, M. S.: Linkages between ocean circulation and the Northeast Greenland Ice Stream in the Early Holocene, Quaternary Sci. Rev., 286, 107530, https://doi.org/10.1016/j.quascirev.2022.107530, 2022.

Dowdeswell, J. A., Ottesen, D., Evans, J., Cofaigh, C. Ó., and Anderson, J. B.: Submarine glacial landforms and rates of ice-stream collapse, Geology, 36, 819–822, https://doi.org/10.1130/G24808A.1, 2008.

Dowdeswell, J. A., Hogan, K. A., Ó Cofaigh, C., Fugelli, E. M. G., Evans, J., and Noormets, R.: Late Quaternary ice flow in a West Greenland fjord and cross-shelf trough system: submarine landforms from Rink Isbrae to Uummannaq shelf and slope, Quaternary Sci. Rev., 92, 292–309, 2014.

Dowdeswell, J. A., Canals, M., Jakobsson, M., Todd, B. J., Dowdeswell, E. K., and Hogan, K. A.: The variety and distribution of submarine glacial landforms and implications for ice-sheet reconstruction, Geol. Soc. Mem., 46, 519–552, https://doi.org/10.1144/M46.183, 2016.

Evans, J., Dowdeswell, J. A., Grobe, H., Niessen, F., Stein, R., Hubberten, H. W., and Whittington, R. J.: Late Quaternary sedimentation in Kejser Franz Joseph Fjord and the continental margin of East Greenland, Geol. Soc. Spec. Publ., 203, 149–179, https://doi.org/10.1144/GSL.SP.2002.203.01.09, 2002.

Evans, J., Ó Cofaigh, C., Dowdeswell, J. A., and Wadhams, P.: Marine geophysical evidence for former expansion and flow of the

Greenland Ice Sheet across the north-east Greenland continental shelf, J. Quaternary Sci., 24, 279–293, 2009.

Eyles, N., Eyles, C. H., and Niall, An. D.: Lithofacies types and vertical profile models; an alternative approach to the description and environmental interpretation of glacial diamict and diamictite sequences, Sedimentology, 30, 393–410, 1983.

Folk, R. L.: The Distinction between Grain Size and Mineral Composition in Sedimentary-Rock Nomenclature, J. Geol., 62, 344–359, 1954.

Folk, R. L. and Ward, W.: Brazos river bar, a study in the significance of grain size parameters, J. Sediment. Petrol., 27, 34–59, 1957.

Forwick, M. and Vorren, T. O.: Deglaciation history and post-glacial mass movements in Balsfjord, northern Norway, Polar Res., 21, 259–266, 1998.

Forwick, M., Vorren, T. O., Hald, M., Korsun, S., Roh, Y., Vogt, C., and Yoo, K. C.: Spatial and temporal influence of glaciers and rivers on the sedimentary environment in Sassenfjorden and Tempelfjorden, Spitsbergen, Geol. Soc. London, Spec. Publ., 344, 163–193, https://doi.org/10.1144/SP344.13, 2010.

Funder, S., Hjort, C., Landvik, J. Y., Nam, S. I., Reeh, N., and Stein, R.: History of a stable ice margin – East Greenland during the middle and upper pleistocene, Quaternary Sci. Rev., 17, 77–123, https://doi.org/10.1016/S0277-3791(97)00082-6, 1998.

Funder, S., Kjeldsen, K. K., Kjær, H. K., and Ó Cofaigh, C.: The Greenland Ice Sheet During the Past 300,000 Years: A Review, Dev. Quat. Sci., 15, 699–713, https://doi.org/10.1016/B978-0-444-53447-7.00050-7, 2011.

Funder, S., Sørensen, A. H. L., Larsen, N. K., Bjørk, A. A., Briner, J. P., Olsen, J., Schomacker, A., Levy, L. B., and Kjær, K. H.: Younger Dryas ice margin retreat in Greenland: new evidence from southwestern Greenland, Clim. Past, 17, 587–601, https://doi.org/10.5194/cp-17-587-2021, 2021.

Geirsdóttir, Á., Hardardóttir, J., and Andrews, J. T.: Late-Holocene terrestrial glacial history of Miki and I.C. Jacobsen Fjords, East Greenland, Holocene, 10, 123–134, https://doi.org/10.1191/095968300666213169, 2000.

Håkansson, L., Graf, A., Strasky, S., Ivy-ochs, S., Kubik, P. W., Hjort, C., Shlüchter, C., Geografiska, S., Series, A., Geography, P., Hakansson, L., Graf, A., Strasky, S., Ivy-ochs, S., Kubik, P. W., Hjort, C., and Schlichter, C.: Cosmogenic 10Be-Ages from the Store Koldewey Island, NE Greenland, Geogr. Ann. A, 89, 195–202, 2007.

Hansen, K. E., Lorenzen, J., Davies, J., Wacker, L., Pearce, C., and Seidenkrantz, M.-S.: Deglacial to Mid Holocene environmental conditions on the northeastern Greenland shelf, Quanternary Sci. Rev., 293, 107704, https://doi.org/10.1016/j.quascirev.2022.107704, 2022.

Heaton, T. J., Köhler, P., Butzin, M., Bard, E., Reimer, R. W., Austin, W. E. N., Ramsey, C. B., Grootes, P. M., Hughen, K. A., Kromer, B., Reimer, P. J., and Heaton, T. J.: Marine20 – The Marine Radiocarbon Age Calibration Curve (0–55,000 cal BP), Radio, 62, 779–820, https://doi.org/10.1017/RDC.2020.68, 2020.

Heaton, T. J., Bard, E., Ramsey, C. B., Butzin, M., Hatté, C., Hughen, K. A., Köhler, P., and Reimer, P. J.: A Response to Community Questions on the Marine20 Radiocarbon Age Calibration Curve: Marine Reservoir Ages and The Calibration of 14C Samples from the Oceans, Radiocarbon, 65, 247–273, https://doi.org/10.1017/RDC.2022.66, 2022.

Higgins, A. K.: North Greenland Glaeier Velocities and Calf Ice Production, Polarforschung, 60, 1–23, 1991.

Hill, P. R.: Changes in submarine channel morphology and strata development from repeat multibeam surveys in the Fraser River delta, western Canada, in: Sediments, Morphology and Sedimentary Processes on Continental Shelves, edited by: Li, M. Z., Sherwood, C. R., and Hill, P. R., Blackwell Science, International Association of Sedimentologists, 47–70, https://doi.org/10.1002/9781118311172.ch3, 2012.

Hjort, C.: Glaciation in northern East Greenland during the Late Weichselian and Early Flandrian, Boreas, 8, 281–296, https://doi.org/10.1111/j.1502-3885.1979.tb00812.x, 1979.

Hjort, C.: A glacial chronology for northern East Greenland, Boreas, 10, 259–274, 1981.

Hjort, C. and Björck, S.: A re-evaluated glacial chronology for Northern East Greenland, Geol. Föreningen i Stock, Förhandlingar, 105, 235–243, https://doi.org/10.1080/11035898309452590, 1983.

Hogan, K. A., Dowdeswell, J. A., Noormets, R., Evans, J., and Ó Cofaigh, C.: Evidence for full-glacial flow and retreat of the Late Weichselian Ice Sheet from the waters around Kong Karls Land, eastern Svalbard, Quaternary Sci. Rev., 29, 3563–3582, https://doi.org/10.1016/j.quascirev.2010.05.026, 2010.

Hogan, K. A., Ó Cofaigh, C., Jennings, A. E., Dowdeswell, J. A., and Hiemstra, J. F.: Deglaciation of a major palaeo-ice stream in Disko Trough, West Greenland, Quaternary Sci. Rev., 147, 5–26, 2016.

Huddart, D. and Lister, H.: The Origin of Ice Marginal Terraces and Contact Ridges of East Kangerdluarssuk Glacier, SW Greenland, Geogr. Ann. A, 63, 31–39, 1981.

Jackson, R., Andreasen, N., Oksman, M., Andersen, T. J., Pearce, C., Seidenkrantz, M.-S., and Ribeiro, S.: Marine conditions and development of the Sirius Water polynya on the North-East Greenland shelf during the Younger Dryas-Holocene, Quaternary Sci. Rev., 291, 107647, https://doi.org/10.1016/j.quascirev.2022.107647, 2022.

Jakobsson, M., Hogan, K. A., Mayer, L. A., Mix, A., Jennings, A., Stoner, J., Eriksson, B., Jerram, K., Mohammad, R., Pearce, C., Reilly, B., and Stranne, C.: The Holocene retreat dynamics and stability of Petermann Glacier in northwest Greenland, Nat. Commun., 9, 2104, https://doi.org/10.1038/s41467-018-04573-2, 2018.

Jakobsson, M., Mayer, L. A., Bringensparr, C., Castro, C. F., Mohammad, R., Johnson, P., Ketter, T., Accettella, D., Amblas, D., An, L., Arndt, J. E., Canals, M., Casamor, J. L., Chauché, N., Coakley, B., Danielson, S., Demarte, M., Dickson, M. L., Dorschel, B., Dowdeswell, J. A., Dreutter, S., Fremand, A. C., Gallant, D., Hall, J. K., Hehemann, L., Hodnesdal, H., Hong, J., Ivaldi, R., Kane, E., Klaucke, I., Krawczyk, D. W., Kristoffersen, Y., Kuipers, B. R., Millan, R., Masetti, G., Morlighem, M., Noormets, R., Prescott, M. M., Rebesco, M., Rignot, E., Semiletov, I., Tate, A. J., Travaglini, P., Velicogna, I., Weatherall, P., Weinrebe, W., Willis, J. K., Wood, M., Zarayskaya, Y., Zhang, T., Zimmermann, M., and Zinglersen, K. B.: The International Bathymetric Chart of the Arctic Ocean Version 4.0, Sci. Data, 7, 1–14, https://doi.org/10.1038/s41597-020-0520-9, 2020.

Joughin, I., Fahnestock, M., MacAyeal, D., Bamber, J. L., and Gogineni, P.: Observation and analysis of ice flow in the largest Green-

land ice stream, J. Geophys. Res.-Atmos., 106, 34021–34034, https://doi.org/10.1029/2001JD900087, 2001.

Kelly, M. A., Lowell, T. V., Hall, B. L., Schaefer, J. M., Finkel, R. C., Goehring, B. M., Alley, R. B., and Denton, G. H.: A 10Be chronology of lateglacial and Holocene mountain glaciation in the Scoresby Sund region, east Greenland: implications for seasonality during lateglacial time, Quaternary Sci. Rev., 27, 2273–2282, 2008.

Kempf, P., Forwick, M., Laberg, J. S., and Vorren, T. O.: Late Weichselian and Holocene sedimentary palaeoenvironment and glacial activity in the high-arctic van Keulenfjorden, Spitsbergen, Holocene, 23, 1607–1618, https://doi.org/10.1177/0959683613499055, 2013.

Khan, S. A., Kjær, K. H., Bevis, M., Bamber, J. L., Wahr, J., Kjeldsen, K. K., Bjørk, A. A., Korsgaard, N. J., Stearns, L. A., Van Den Broeke, M. R., Liu, L., Larsen, N. K., and Muresan, I. S.: Sustained mass loss of the northeast Greenland ice sheet triggered by regional warming, Nat. Clim. Change, 4, 292–299, https://doi.org/10.1038/nclimate2161, 2014.

King, E. C., Hindmarsh, R. C. A., and Stokes, C. R.: Formation of mega-scale glacial lineations observed beneath a West Antarctic ice stream, Nat. Geosci., 2, 585–588, https://doi.org/10.1038/ngeo581, 2009.

King, M. D., Howat, I. M., Candela, S. G., Noh, M. J., Jeong, S., Noël, B. P. Y., van den Broeke, M. R., Wouters, B., and Negrete, A.: Dynamic ice loss from the Greenland Ice Sheet driven by sustained glacier retreat, Commun. Earth Environ., 1, 1–7, https://doi.org/10.1038/s43247-020-0001-2, 2020.

Klages, J. P., Kuhn, G., Hillenbrand, C.-D., Graham, A. G. C., Smith, J. A., Larter, R. D., and Gohl, K.: First geomorphological record and glacial history of an inter-ice stream ridge on the West Antarctic continental shelf, Quaternary Sci. Rev., 61, 47–61, 2013.

Klages, J. P., Kuhn, G., Graham, A. G. C., Hillenbrand, C.-D., Smith, J. A., Nitsche, F. O., Larter, R. D., and Gohl, K.: Palaeo-ice stream pathways and retreat style in the easternmost Amundsen Sea Embayment, West Antarctica, revealed by combined multibeam bathymetric and seismic data, Geomorphology, 245, 207–222, 2015.

Klug, M., Schmidt, S., Melles, M., Wagner, B., Bennike, O., and Heiri, O.: Lake sediments from Store Koldewey, Northeast Greenland, as archive of Late Pleistocene and Holocene climatic and environmental changes, Boreas, 38, 59–71, https://doi.org/10.1111/j.1502-3885.2008.00038.x, 2009a.

Klug, M., Bennike, O., and Wagner, B.: Repeated short-term bioproductivity changes in a coastal lake on Store Koldewey, northeast Greenland: An indicator of varying sea-ice coverage?, Holocene, 19, 653–663, https://doi.org/10.1177/0959683609104040, 2009b.

Klug, M., Bennike, O., and Wagner, B.: Late Pleistocene to early Holocene environmental changes on Store Koldewey, coastal north-east Greenland, Polar Res., 35, 21912, https://doi.org/10.3402/polar.v35.21912, 2016.

Kobashi, T., Menviel, L., Jeltsch-Thömmes, A., Vinther, B. M., Box, J. E., Muscheler, R., Nakaegawa, T., Pfister, P. L., Döring, M., Leuenberger, M., Wanner, H., and Ohmura, A.: Volcanic influence on centennial to millennial Holocene Greenland temperature change, Sci. Rep., 7, 1–10, https://doi.org/10.1038/s41598-017-01451-7, 2017.

Kolling, H. M., Stein, R., Fahl, K., Perner, K., and Moros, M.: Short-term variability in late Holocene sea ice cover on the East Greenland Shelf and its driving mechanisms, Palaeogeogr. Palaeocl., 485, 336–350, https://doi.org/10.1016/j.palaeo.2017.06.024, 2017.

Krieger, L., Floricioiu, D., and Neckel, N.: Drainage basin delineation for outlet glaciers of Northeast Greenland based on Sentinel-1 ice velocities and TanDEM-X elevations, Remote Sens. Environ., 237, 111483, https://doi.org/10.1016/j.rse.2019.111483, 2020.

Laberg, J. S., Forwick, M., and Husum, K.: New geophysical evidence for a revised maximum position of part of the NE sector of the Greenland ice sheet during the last glacial maximum, Arktos, 3, 1–9, https://doi.org/10.1007/s41063-017-0029-4, 2017.

Lambeck, K., Rouby, H., Purcell, A., Sun, Y., and Sambridge, M.: Sea level and global ice volumes from the Last Glacial Maximum to the Holocene, P. Natl. Acad. Sci. USA, 111, 15296–15303, https://doi.org/10.1073/pnas.1411762111, 2014.

Landvik, J. Y.: The last glaciation of Germania Land and adjacent areas, northeast Greenland, J. Quaternary Sci., 9, 81–92, https://doi.org/10.1002/jqs.3390090108, 1994.

Lane, T. P., Roberts, D. H., Ó Cofaigh, C., Vieli, A., and Moreton, S. G.: The glacial history of the southern Svartenhuk Halvø, West Greenland, Arktos, 1, 1–28, https://doi.org/10.1007/s41063-015-0017-5, 2015.

Larsen, N. K., Funder, S., Linge, H., Möller, P., Schomacker, A., Fabel, D., Xu, S., and Kjær, K. H.: A Younger Dryas re-advance of local glaciers in north Greenland, Quaternary Sci. Rev., 147, 47–58, https://doi.org/10.1016/j.quascirev.2015.10.036, 2016.

Larsen, N. K., Søndergaard, A. S., Levy, L. B., Olsen, J., Strunk, A., Bjørk, A. A., and Skov, D.: Contrasting modes of deglaciation between fjords and inter-fjord areas in eastern North Greenland, Boreas, 49, 905–919, https://doi.org/10.1111/bor.12475, 2020.

Larsen, N. K., Søndergaard, A. S., Levy, L. B., Strunk, A., Skov, D. S., Bjørk, A., Khan, S. A., and Olsen, J.: Late glacial and Holocene glaciation history of North and Northeast Greenland, Arct. Antarct. Alp. Res., 54, 294–313, https://doi.org/10.1080/15230430.2022.2094607, 2022.

Lecavalier, B. S., Milne, G. A., Simpson, M. J. R., Wake, L., Huybrechts, P., Tarasov, L., Kjeldsen, K. K., Funder, S., Long, A. J., Woodroffe, S., Dyke, A. S., and Larsen, N. K.: A model of Greenland Ice Sheet deglaciation constrained by observations of relative sea level and ice extent, Quaternary Sci. Rev., 102, 54–84, 2014.

Levy, L. B., Kelly, M. A., Lowell, T. V., Hall, B. L., Howley, J. A., and Smith, C. A.: Coeval fluctuations of the Greenland ice sheet and a local glacier, central East Greenland, during late glacial and early Holocene time, Geophys. Res. Lett., 43, 1623–1631, 2016.

Lyså, A. and Vorren, T. O.: Seismic facies and architecture of ice-contact submarine fans in high-relief fjords, Troms, Northern Norway, Boreas, 26, 309–328, 1997.

Mouginot, J., Rignot, E., Scheuchl, B., Fenty, I., Khazendar, A., Morlighem, M., Buzzi, A., and Paden, J.: Fast retreat of Zachariae Isstrom, Northeast Greenland, Science, 350, 1357–1361, 2015.

Mouginot, J., Bjørk, A. A., Millan, R., Scheuchl, B., and Rignot, E.: Insights on the Surge Behavior of Storstrømmen and L. Bistrup Bræ, Northeast Greenland, Over the Last Century, Geophys. Res.

Lett., 45, 11197–11205, https://doi.org/10.1029/2018GL079052, 2018.

Newton, A. M. W., Knutz, P. C., Huuse, M., Gannon, P., Brocklehurst, S. H., Clausen, O. R., and Gong, Y.: Ice stream reorganization and glacial retreat on the northwest Greenland shelf, Geophys. Res. Lett., 44, 7826–7835, https://doi.org/10.1002/2017GL073690, 2017.

Ó Cofaigh, C.: Flow Dynamics and till genesis associated with a marin-based Antarctic palaeo-ice stream, Quaternary Sci. Rev., 24, 709–740, 2005.

Ó Cofaigh, C., Dowdeswell, J. A., and Grobe, H.: Holocene glacimarine sedimentation, inner Scoresby Sund, East Greenland: The influence of fast-flowing ice-sheet outlet glaciers, Mar. Geol., 175, 103–129, https://doi.org/10.1016/S0025-3227(01)00117-7, 2001.

Ó Cofaigh, C., Dowdeswell, J. A., Jennings, A. E., Hogan, K. A., Kilfeather, A., Hiemstra, J. F., Noormets, R., Evans, J., McCarthy, D. J., Andrews, J. T., Lloyd, J. M., and Moros, M.: An extensive and dynamic ice sheet on the west greenland shelf during the last glacial cycle, Geology, 41, 219–222, https://doi.org/10.1130/G33759.1, 2013.

Olsen, I. L., Rydningen, T. A., Forwick, M., Laberg, J. S., and Husum, K.: Last glacial ice sheet dynamics offshore NE Greenland – a case study from Store Koldewey Trough, The Cryosphere, 14, 4475–4494, https://doi.org/10.5194/tc-14-4475-2020, 2020.

Olsen, I. L., Laberg, J. S., Forwick, M., Rydningen, T. A., and Husum, K.: Late Weichselian and Holocene behavior of the Greenland Ice Sheet in the Kejser Franz Josef Fjord system, NE Greenland, Quaternary Sci. Rev., 284, 107504, https://doi.org/10.1016/j.quascirev.2022.107504, 2022.

ORAU (Oxford Radiocarbon Accelerator Unit): OxCal Online, Version 4.4, https://c14.arch.ox.ac.uk/oxcal.html#program (last access: 5 April 2023), 2022.

Ottesen, D., Dowdeswell, J. A., and Rise, L.: Submarine landforms and the reconstruction of fast-flowing ice streams within a large Quaternary ice sheet: The 2500-km-long Norwegian-Svalbard margin (57°–80° N), Bull. Geol. Soc. Am., 117, 1033–1050, https://doi.org/10.1130/B25577.1, 2005.

Ottesen, D., Dowdeswell, J. A., Benn, D. I., Kristensen, L., Christiansen, H. H., Christensen, O., Hansen, L., Lebesbye, E., Forwick, M., and Vorren, T. O.: Submarine landforms characteristic of glacier surges in two spitsbergen fjords, Quaternary Sci. Rev., 27, 1583–1599, 2008.

Pados-Dibattista, T., Pearce, C., Detlef, H., Bendtsen, J., and Seidenkrantz, M.-S.: Holocene palaeoceanography of the Northeast Greenland shelf, Clim. Past, 18, 103–127, https://doi.org/10.5194/cp-18-103-2022, 2022.

Pedersen, J. B. T., Kroon, A., and Jakobsen, B. H.: Holocene sea-level reconstruction in the Young Sound region, Northeast Greenland, J. Quaternary Sci., 26, 219–226, 2011.

Rahmstorf, S., Box, J. E., Feulner, G., Mann, M. E., Robinson, A., Rutherford, S., and Schaffernicht, E. J.: Exceptional twentieth-century slowdown in Atlantic Ocean overturning circulation, Nat. Clim. Change, 5, 475–480, https://doi.org/10.1038/nclimate2554, 2015.

Rasmussen, T. L., Pearce, C., Andresen, K. J., Nielsen, T., and Seidenkrantz, M.-S.: Northeast Greenland: ice-free shelf edge at 79.4° N around the Last Glacial Maximum 25.5–17.5 ka, Boreas, 51, 759–775, 2022.

Reeh, N., Bøggild, C. E., and Oerter, H.: Surge of Storstrømmen, a large outlet glacier from the Inland Ice of North-East Greenland, Rapp. Grønands Geol. Unders., 162, 201–209, 1994.

Reilly, B. T., Stoner, J. S., Mix, A. C., Walczak, M. H., Jennings, A., Jakobsson, M., Dyke, L., Glueder, A., Nicholls, K., Hogan, K. A., Mayer, L. A., Hatfield, Robert, G., Albert, S., Marcott, S., Fallon, S., and Cheseby, M.: Holocene break-up and reestablishment of the Petermann Ice Tongue, Northwest Greenland, Quaternary Sci. Rev., 218, 322–342, 2019.

Reimer, P. J., Austin, W. E. N., Bard, E., Bayliss, A., Blackwell, P. G., Bronk Ramsey, C., Butzin, M., Cheng, H., Edwards, R. L., Friedrich, M., Grootes, P. M., Guilderson, T. P., Hajdas, I., Heaton, T. J., Hogg, A. G., Hughen, K. A., Kromer, B., Manning, S. W., Muscheler, R., Palmer, J. G., Pearson, C., Van Der Plicht, J., Reimer, R. W., Richards, D. A., Scott, E. M., Southon, J. R., Turney, C. S. M., Wacker, L., Adolphi, F., Büntgen, U., Capano, M., Fahrni, S. M., Fogtmann-Schulz, A., Friedrich, R., Köhler, P., Kudsk, S., Miyake, F., Olsen, J., Reinig, F., Sakamoto, M., Sookdeo, A., and Talamo, S.: The IntCal20 Northern Hemisphere Radiocarbon Age Calibration Curve (0–55 cal kBP), Radiocarbon, 62, 725–757, https://doi.org/10.1017/RDC.2020.41, 2020.

Rignot, E., Bjork, A., Chauche, N., and Klaucke, I.: Storstrømmen and L. Bistrup Bræ, North Greenland, Protected From Warm Atlantic Ocean Waters, Geophys. Res. Lett., 49, e2021GL097320, https://doi.org/10.1029/2021GL097320, 2022.

Sættem, J.: Glaciotectonic forms and structures on the Norwegian continental shelf: observations, processes and implications, Nor. Geol. Tidsskr., 70, 81–94, 1990.

Schaffer, J., von Appen, W.-J., Dodd, P. A., Hofstede, C., Mayer, C., de Steur, L., and Kanzow, T.: Warm water pathways toward Nioghalvfjerdsfjorden Glacier, Northeast Greenland, J. Geophys. Res.-Oceans, 122, 4004–4020, https://doi.org/10.1002/2016JC012462, 2017.

Schmidt, S., Wagner, B., Heiri, O., Klug, M., Bennike, O., and Melles, M.: Chironomids as indicators of the Holocene climatic and environmental history of two lakes in Northeast Greenland, Boreas, 40, 116–130, https://doi.org/10.1111/j.1502-3885.2010.00173.x, 2011.

Schoof, C. G. and Clarke, G. K. C.: A model for spiral flows in basal ice and the formation of subglacial flutes based on a Reiner-Rivlin rheology for glacial ice, J. Geophys. Res.-Sol. Ea., 113, B05204, https://doi.org/10.1029/2007JB004957, 2008.

Shaw, J., Pugin, A., and Young, R. R.: A meltwater origin for Antarctic shelf bedforms with special attention to megalineations, Geomorphology, 102, 364–375, https://doi.org/10.1016/j.geomorph.2008.04.005, 2008.

Shreve, R. L.: Esker characteristics in terms of glacier physics, Katahdin esker system, Maine, Geol. Soc. Am. Bull., 96, 639–646, https://doi.org/10.1130/0016-7606(1985)96<639:ECITOG>2.0.CO;2, 1985.

Skov, D. S., Andersen, J. L., Olsen, J., Jacobsen, B. H., Knudsen, M. F., Jansen, J. D., Larsen, N. K., and Egholm, D. L.: Constraints from cosmogenic nuclides on the glaciation and erosion history of Dove Bugt, northeast Greenland, GSA Bull., 132, 1–13, 2020.

Slabon, P., Dorschel, B., Jokat, W., Myklebust, R., Hebbeln, D., and Gebhardt, C.: Greenland ice sheet retreat history in the northeast Baffin Bay based on high-

resolution bathymetry, Quaternary Sci. Rev., 154, 182–198, https://doi.org/10.1016/j.quascirev.2016.10.022, 2016.

Smith, L. M. and Andrews, J. T.: Sediment characteristics in iceberg dominated fjords, Kangerlussuaq region, East Greenland, Sediment. Geol., 130, 11–25, https://doi.org/10.1016/S0037-0738(99)00088-3, 2000.

Stacey, C. D. and Hill, P. R.: Cyclic steps on a glacifluvial delta, Howe Sound, British Columbia, in: Atlas of Submarine Glacial Landforms: Modern, Quaternary and Ancient, edited by: Dowdeswell, J. A., Canals, M., Jakobsson, M., Todd, B. J., Dowdeswell, E. K., and Hogan, K. A., Geological Society of London, 93–94, ISBN 9781786202680, 2016.

Stocker, T. F., Qin, D., Plattner, G.-K., Tignor, M. M. B., Allen, S. K., Boschung, J., Nauels, A., Xia, Y., Bex, V., and Midgley, P. M.: Climate Change 2013: The Physical Science Basis, Contribution of Working Group I to the Fifth Assessment Report of the Intergovernmental Panel on Climate Change, Cambridge, https://doi.org/10.1017/CBO9781107415324, 2013.

Stokes, C. R. and Clark, C. D.: Geomorphological criteria for identifying Pleistocene ice streams, Ann. Glaciol., 28, 67–74, https://doi.org/10.3189/172756499781821625, 1999.

Stokes, C. R. and Clark, C. D.: Palaeo-ice streams, Quaternary Sci. Rev., 20, 1437–1457, 2001.

Storrar, R. D., Stokes, C. R., and Evans, D. J. A.: Morphometry and pattern of a large sample (> 20,000) of Canadian eskers and implications for subglacial drainage beneath ice sheets, Quaternary. Sci. Rev., 105, 1–25, https://doi.org/10.1016/j.quascirev.2014.09.013, 2014.

Syring, N., Lloyd, J. M., Stein, R., Fahl, K., Roberts, D. H., Callard, L., and O'Cofaigh, C.: Holocene interactions between glacier retreat, sea ice formation, and Atlantic water advection at the inner Northeast Greenland continental shelf, Paleoceanogr. Paleoclimatology, 35, e2020PA004019, https://doi.org/10.1029/2020PA004019, 2020.

Vasskog, K., Langebroek, P. M., Andrews, J. T., Nilsen, J. E. Ø., and Nesje, A.: The Greenland Ice Sheet during the last glacial cycle: Current ice loss and contribution to sea-level rise from a palaeoclimatic perspective, Earth-Sci. Rev., 150, 45–67, https://doi.org/10.1016/j.earscirev.2015.07.006, 2015.

Wagner, B., Bennike, O., Bos, J. A. A., Cremer, H., Lotter, A. F., and Melles, M.: A multidisciplinary study of Holocene sediment records from Hjort Sø on Store Koldewey, Northeast Greenland, J. Paleolimnol., 39, 381–398, https://doi.org/10.1007/s10933-007-9120-3, 2008.

Weber, M. E., Niessen, F., Kuhn, G., and Wiedicke, M.: Calibration and application of marine sedimentary physical properties using a mult-sensor core logger, Mar. Geol., 136, 151–172, 1997.

Weidick, A., Andreasen, C., Oerter, H., and Reeh, N.: Neoglacial glacier changes around Storstrommen, north-east Greenland, Polarforschung, 64, 95–108, 1994.

Wilson, N. J. and Straneo, F.: Water exchange between the continental shelf and the cavity beneath Nioghalvfjerdsbræ (79 North Glacier), Geophys. Res. Lett., 42, 7648–7654, https://doi.org/10.1002/2015GL064944, 2015.

Winkelmann, D., Jokat, W., Jensen, L., and Schenke, H. W.: Submarine end moraines on the continental shelf off NE Greenland – Implications for Lateglacial dynamics, Quaternary Sci. Rev., 29, 1069–1077, https://doi.org/10.1016/j.quascirev.2010.02.002, 2010.

Zoller, K., Laberg, J. S., and Rydningen, T. A.: Supporting Data for: A high-Arctic inner shelf–fjord system from the Last Glacial Maximum to the Present: Bessel Fjord and SW Dove Bugt, NE Greenland, DataverseNO [data set], https://doi.org/10.18710/IXW3VA, 2022.